THESIS FOR THE DEGREE OF DOCTOR OF PHILOSOPHY

Ship-Bridge Allision Risk Analysis

AIS-based Failure Event Modelling and Consequence Assessment

AXEL HÖRTEBORN

Department of Mechanics and Maritime Sciences
CHALMERS UNIVERSITY OF TECHNOLOGY
Gothenburg, Sweden 2025

Ship-Bridge Allision Risk Analysis
AIS-based Failure Event Modelling and Consequence Assessment
AXEL HÖRTEBORN
ISBN: 978-91-8103-315-1

Doktorsavhandlingar vid Chalmers tekniska högskola
Series number: 5772
ISSN: 0346-718X

Chalmers University of Technology
Department of Mechanics and Maritime Sciences
Division of Marine Technology
SE-412 96, Gothenburg
Sweden
Telephone: + 46 (0)31-772 1000

Printed by Chalmers Reproservice
www.chalmers.se
Gothenburg, Sweden 2025

Ship-Bridge Allision Risk Analysis
AXEL HÖRTEBORN
Chalmers University of Technology
Department of Mechanics and Maritime Sciences
Division of Marine Technology

Abstract

Increases in ship sizes and in maritime traffic frequency pose a growing risk of ship-bridge allisions. Although relatively rare, such accidents can have catastrophic consequences, including significant economic disruption and loss of life. However, constructing robust bridges capable of withstanding allisions with large ships travelling at high speeds is costly. Therefore, to balance risk and expense, it is crucial to conduct a thorough risk assessment. Traditional risk assessment methodologies often separate the probability analysis from the consequence analysis, but this separation leads to generalisation, less accuracy, and the introduction of overly conservative assumptions, and it may not reflect local traffic patterns or ship manoeuvring failure behaviours. This thesis aims to develop a novel, unified analysis for assessing the risk of ship-bridge allisions by integrating local ship manoeuvring failure statistics, probabilistic modelling, and consequence analysis into a single methodology.

The thesis presents the four stages of the development of a new methodology, STAPS-cons (Ship Traffic Allision Probability using Simulations – consequences). First, five distinct types of ship manoeuvring failure were identified based on Automatic Identification System (AIS) data: (1) loss of propulsion; (2) loss of steering; (3) miss of turning point; (4) wrong course at a turning point; and (5) turn at the wrong location. These failure types were also quantified with respect to frequency and duration, using a combination of trajectory analysis and manual classification. In the second stage, millions of input datasets were generated in a Monte Carlo simulation based on a combination of these failures, environmental parameters, and ship statistics. In the third stage, these inputs were simulated in a time-domain hydrodynamic simulator to model the ship behaviour under respective failure conditions. The number of simulations was determined based on route-specific traffic volumes and failure probabilities. In the final stage, the consequences of failures leading to allisions were analysed using a set of precalculated nonlinear finite element analyses, enabling the estimation of structural damage and collapse probability. The thesis focuses on energy transfer and bridge collapse probability; socioeconomic consequences (e.g., loss of life, or traffic disruptions) fall outside its scope.

The results presented in the thesis demonstrate that the STAPS-cons methodology provides a more detailed and realistic assessment of ship-bridge allision risk than existing models. The methodology also includes real-time replays for identification of high-risk scenarios and evaluation of risk mitigation strategies. The methodology was applied in multiple case studies and compared with established tools (e.g., IWRAP Mk II), wherein it showed comparable or better performance. Future work includes broadening the scope to include analysing offshore wind farms and the probability of ship groundings, automating failure classification and future route paths using AI, and developing fast-time consequence approximations to reduce the need for time-consuming finite element modelling. Overall, STAPS-cons represents a significant advancement in maritime risk assessment by combining probability and consequence modelling in a flexible, simulation-based methodology.

Keywords: AIS data, navigation failure statistics, risk analysis, ship manoeuvring simulations.

Preface

This thesis is comprised of research work carried out in the years 2017–2025 at the Maritime Department at RISE (formerly SSPA) and the Division of Marine Technology in the Department of Mechanics and Maritime Sciences at the Chalmers University of Technology. I'm very grateful for the financial support that I received for this research from the Swedish Transport Administration, the Norwegian Public Road Administration, and my employer RISE.

I would like to express my gratitude to my examiner and head supervisor, Professor Jonas W. Ringsberg, for all his feedback and his dedication to improving my skills. I also want to thank my assistant supervisors, Professor Wengang Mao and Doctor Olov Lundbäck, for all their feedback during this journey.

Furthermore, I would like to thank my friend Erik Iveroth, who—over a couple of bottles of red wine—taught me the programming language Python, a language I have used throughout my research. I also want to thank my former colleague Henrik Holm, who taught me SQL and who set up the AIS database structure which has been used in this research. Erland Wilske and Björn Forsman, thank you for the start and all the work we did as a team in my first years at SSPA related to the *Björnafjorden project*, which initiated the demand for this research. Also, I'm very grateful to the entire team at the Maritime Department at RISE, where I've gained an understanding of operations at sea.

In addition to the invaluable support and guidance I have received, I am deeply honoured by the international recognition which my research has attracted. It was a proud moment for me to be awarded second place in the PIANC De Paepe-Willems Award for 2025 for a paper in which I applied the developed methodology to assess the probability of allision for ten different bridges across the United States. The acknowledgement from the global maritime community is both humbling and motivating, and it reinforces the value and applicability of the work undertaken in this thesis.

Finally, I could never have done this without the unconditional love and support from my family. Algot and Ester, my wonderful kids, always so full of energy and curiosity! I am especially thankful to my amazing wife, Doctor Hörteborn (I soon hope that we are two).

Axel Hörteborn
Varberg, November 2025

Table of Contents

List of appended papers

For each of the four appended papers, the author of this thesis contributed to the presented ideas, planned the paper with the co-authors, performed the numerical simulations, and wrote the manuscript with the co-authors.

Paper I Hörteborn, A., Ringsberg, J.W., 2021. A method for risk analysis of ship collisions with stationary infrastructure using AIS data and a ship manoeuvring simulator. *Ocean Engineering*, 235 (September 2021), 109396. https://doi.org/10.1016/j.oceaneng.2021.109396.

Paper II Hörteborn, A., Eidem, M.E., 2025. Probability of active navigational failures. Accepted by *The Journal of Navigation*. https://doi.org/10.1017/S0373463325101100. (Accepted, available online 2025-11-01.)

Paper III Hörteborn, A., Ringsberg, J.W., Lundbäck, O., Mao, W., 2025. Probabilistic analysis of ship-bridge allisions when designing bridges. *Reliability Engineering & System Safety*, 260, (August 2025), 111026. https://doi.org/10.1016/j.ress.2025.111026.

Paper IV Hörteborn, A., Sha, Y., Ringsberg, J.W., Lundbäck, O., Mao, W. 2025. Risk analysis methodology for ship-bridge allisions – A combined probability and consequence analysis. (Accepted for publication in *Engineering Structures*.)

Authors' contribution (CRediT)

Axel Hörteborn	Conceptualization, Methodology, Software, Validation, Formal analysis, Investigation, Data curation, Visualization, Resources, Writing—Original Draft, Writing—Review & Editing, Funding acquisition, Project administration (Papers I – IV).
Jonas W. Ringsberg	Writing—Review & Editing, Supervision, Conceptualization Methodology, Project administration (Papers I, III – IV)
Mathias E. Eidem	Conceptualization, Methodology, Investigation, Writing–Review & Editing (Paper II)
Olov Lundbäck	Writing—Review & Editing, Supervision, Software, Conceptualization, Methodology (Papers III – IV)
Wengang Mao	Writing—Review & Editing, Supervision, Conceptualization, Methodology (Papers III – IV)
Yanyan Sha	FE modelling and analysis, Investigation, Data curation, Writing—Review & Editing (Paper IV)

List of other published papers by the author

Paper A Svanberg, M., Santén, V., Hörteborn, A., Holm, H., Finnsgård, C., 2019. AIS in maritime research. Marine Policy 106, 103520. https://doi.org/10.1016/j.marpol.2019.103520.

Paper B Andersson, A. (NKA Hörteborn A.), Forsman, B., Wilske, E., 2016. Estimation of ship bridge collision probability by use of Monte Carlo simulations. Challenges in Design and Construction of an Innovative and Sustainable Built Environment: IABSE Congress, 21-23 September 2016, Stockholm, Sweden, pp. 142-149, IABSE - International Association for Bridge and Structural Engineering, Zürich, Switzerland. ISBN: 978-3-85748-144-4. https://doi.org/10.2749/stockholm.2016.0142.

Paper C Hörteborn, A., Ringsberg, J.W., Svanberg, M., Holm, H., 2019. A revisit of the definition of the ship domain based on AIS analysis. The Journal of Navigation 72(3), pp.777-794. https://doi.org/10.1017/S0373463318000978.

Paper D Hörteborn, A., Ringsberg, J.W., Svanberg, M., 2019. A comparison of two definitions of ship domain for analysing near ship–ship collisions, in: Developments in the Collision and Grounding of Ships and Offshore Structures: Proceedings of the 8th International Conference on Collision and Grounding of Ships and Offshore Structures (ICCGS 2019), 21-23 October, 2019, Lisbon, Portugal. CRC Press, p. 308-315. https://doi.org/10.1201/9781003002420.

Paper E Hörteborn, A. Hassellöv, I., 2023. Economic incentives and technological limitations govern environmental impact of LNG feeder vessels. Journal of Cleaner Production 429, 139461. https://doi.org/10.1016/j.jclepro.2023.139461.

Paper F Hörteborn, A., 2024. Allision modelling in IWRAP Mk II – A verification and sensitivity study. Proceedings of the 9th International Conference on Collision and Grounding of Ships and Offshore Structures (ICCGS 2023), 11-13 September, 2023, Nantes, France. CRC Press, p. 51-59. https://doi.org/10.1201/9781003462170.

Paper G Hörteborn, A., 2026. Probability for Ship-Bridge Allisions in the USA. De Paepe-Willems Award. To be published in the PIANC Yearbook 2025. https://www.pianc.org/wp-content/uploads/2025/05/Axel-Horteborn.pdf (Available online 2025-11-01).

Nomenclature

Greek notations

α	Impact angle between the ship and structure surfaces [degrees]
β	Impact angle between the ship travel direction and the pontoon direction [degrees]
δ_1	Upper bound of the critical approach angle that could result in an allision [degrees]
δ_2	Lower bound of the critical approach angle that could result in an allision [degrees]
τ	Location [-]
λ	Scale [-]
μ	Mean value [h] or [s]
σ	Standard deviation [-]

Latin notations

A_i	Expected number of allisions during the design period
AF	Annual frequency of bridge element collapse
C_g	Global maximum capacity [MJ]
C_l	Local maximum capacity [MJ]
D_G	Geometrical distribution of vessel courses
D_{sc}	Displacement of the ship [m^3]
$E_{int, ship}$	Internal structural deformation energy used by the ship [MJ]
$E_{int, structure}$	Internal structural deformation energy used by the structure [MJ]
F_{dyn}	Impact force of the allision in the Eurocode [J]
fp	Failure probability per unit of travel distance
ft	Index denoting failure type [-]
i	Index denoting the seed number used in the Monte Carlo simulation [-]
K_0	Kinetic energy of the ship prior to impact [MJ]
k_{DC}	Distance compensation factor [-]
$K_{bridge, ship}$	Kinetic energy of the bridge after impact [MJ]
$K_{pos, ship}$	Kinetic energy of the ship after impact [MJ]
k_{RR}	Risk reduction factor [-]
L	Route length [m]
M_{sim}	Number of simulations to run [-]
N_a	Number of accidents [-]
$N_{r,sc}$	Estimated number of ships per year for ship type *j* on a route *k* in the area [-]
$N_{collapse}$	Total number of collapses [-]
N_G	Number of geometrical candidates
N_{sim}	Number of simulations to run [-]
N_{turns}	Number of turns per route [-]
p_a	Human intervention factor in the Eurocode [-]
PA	Probability of vessel aberrancy in AASHTO [event/hour]
PC	Probability of collapse due to a bridge allision in AASHTO [event/allision]
P_C	Failure probability in the Eurocode and in Eq. (2.1) [failure/hour]
PF	Adjustment factor to compensate for potential mitigations in AASHTO [-]
PG	Geometric probability in AASHTO [vessels/hour]

P_{ft}	Failure probability per hour for the failure type ft [1/hour]
R	Structural resistance used in Eurocode [J]
r	Index denoting route number [-]
sc	Index denoting ship category [-]
T	Reference period used in Eurocode [Years]
u	Velocity in side direction [m/s]
v	Velocity in forward direction [m/s]
z	Position of where the failure occurs in Eurocode [m]
Y_{rep}	Number of repetitions of one-year's traffic represented [-]
$W_{hyd, ship}$	Work done by hydrodynamic forces of the ship [MJ]
$W_{hyd, structure}$	Work done by hydrodynamic forces of the structure [MJ]
W_{fri}	Work done by the friction in the allision [MJ]

Abbreviations

AASHTO	American Association of State Highway and Transportation Officials
AtoN	Aids to Navigation
AIS	Automatic Identification System
COG	Course Over Ground
CG	Centre of Gravity
DMTS	Dynamic Maritime Traffic Simulator
DOF	Degrees of Freedom
ESMN	European Maritime Simulator Network
FSA	Formal Safety Assessment
FEA	Finite Element Analysis
IABSE	International Association for Bridge and Structural Engineering
IALA	International Association of Marine Aids to Navigation and Lighthouse Authorities
IMO	International Maritime Organization
MASS	Maritime Autonomous Surface Ship
MMS	Maritime Manoeuvring Simulator
MMSI	Maritime Mobile Service Identity
MTS	Maritime Transportation System
nm	nautical mile
NMEA	National Marine Electronics Association
NPRA	Norwegian Public Road Administration
OMRAT	Open Maritime Risk Analysis Tool
SOLAS	Safety of Life at Sea
SOG	Speed Over Ground
SQL	Structured Query Language
STAPS	Ship Traffic Allision Probability using Monte Carlo Simulations
STAPS-cons	Ship Traffic Allision Probability using Monte Carlo Simulations – consequence
TSS	Traffic Separation Schema
TWL	Turn at the Wrong Location
VTS	Vessel Traffic Service
WCT	Wrong course at a turning point

1 Introduction

Increases in both maritime traffic and ship sizes over recent decades has raised the danger to existing maritime structures, such as quays and bridges. This risk was exemplified on 26 March 2024, when the vessel DALI struck the Francis Scott Key Bridge in Baltimore (NTSB, 2024); six people lost their lives in the accident, and the bridge collapsed, causing a major disruption to the busy port and in the city's transport infrastructure. In this thesis, this type of accident—i.e., between a ship and a built structure—is distinguished from ship-to-ship accidents, with the former termed an allision and the latter termed a collision. These two types of accidents differ fundamentally: in an allision, it is mainly one vessel's decisions which can lead to or prevent an accident, whereas in a collision, two vessels are involved, which drastically increases the complexity of the situation.

The research presented in this thesis was initiated as part of the Norwegian E39 project, which aimed to establish a continuous coastal highway route between Kristiansand and Trondheim in Norway. This route includes seven fjord crossings, which are currently operated by ferries; for several of the crossings, the volume of ship traffic and the associated allision risk present significant challenges. One of the most complex crossings traverses Bjørnafjorden, which spans 5 km and reaches depths of over 500 metres. According to Bjøndal et al. (2016), three different crossing solutions were initially considered: a tension leg platform bridge, a submerged floating tunnel, and a floating bridge. Analysing the allision risks for these solutions necessitated the development of new and innovative models and methods. Accordingly, the following sections provide the background and motivation for this research.

1.1 Background and motivation

Over the past century, maritime traffic has increased substantially, both in terms of the number and the size of vessels. Simultaneously, the global road network has vastly expanded to incorporate numerous bridges spanning waterways. Reliable infrastructure is a cornerstone of economic growth, but bridge construction is costly; for example, the Öresund Bridge cost 44 billion SEK[1] (Persson and Rosengren, 2000), and the Francis Scott Key Bridge cost 8.3 billion SEK[1] (New York Times, 1977). Although the rebuilding cost of the Francis Scott Key Bridge is not yet known, estimates range between 17 and 31 billion SEK (AP News, 2024; NBC4, 2024). These figures are substantial, yet they represent only a fraction of the societal costs of a bridge failure, which are incurred when tens of thousands of vehicles are forced to take multi-hour detours every day.

[1] Based on an average inflation of 3.75% to 2025 and an exchange rate of 10SEK/1USD.

One of the main objectives in risk analysis for bridges spanning navigational waters is to find an optimal balance between construction costs and survival of a potential ship-bridge allision. Such risk analyses are important for guiding infrastructure investments and enforcing safety measures. In practice, risk analyses are typically divided into an assessment of probability, which addresses how likely an accident is to occur, and an assessment of consequences, which evaluates the potential impact should an accident happen. Recent reviews of the methods for maritime risk analysis by Čorić et al. (2021), Galić et al. (2022), and Xiao et al. (2022) have highlighted that current methods for assessing allision probability are often based on theories developed by Fujii and Shiobara (1971), Fujii and Tanaka (1971), and Macduff (1974), and later extended by Pedersen (1995); however, when Fujii and Macduff pioneered the research field of maritime risk analysis, ship movements were typically estimated using radar image records. Svanberg et al. (2019) pointed out that the introduction of the Automatic Identification System (AIS) in the early 2000s and the subsequent availability of AIS data have opened up new possibilities for improving the accuracy of maritime risk assessments. However, the exploitation of the potential to capture ship failure statistics has been rather limited in the academic literature.

Research on the consequences of ship-structure allisions started with the pioneer Minorsky (1958), who investigated the relationship between a ship's kinetic energy and the deformation volume in ship-ship collisions. The structural deformation mechanism was further studied by Amdahl (1983), among others, and Pedersen (1995) subsequently developed the equations applied in maritime risk analysis. These consequence assessments have significantly advanced in the last decade, particularly through high-fidelity finite element analysis (FEA) models, as demonstrated by Le Sourne et al. (2012), Sha et al. (2019a), and Chen et al. (2024). A more in-depth review of the state-of-the-art in the research fields of probability and consequences assessments is found in Chapter 2.

Another aspect which has changed since Fujii and Shiobara (1971) and Macduff (1974) began assessing maritime accident probabilities is computational capacity. Moore (1965) predicted that computing power would double approximately every two years, and this trend has enabled the development of new and innovative methodologies for estimating the risk of ship allisions. As outlined above, risk assessments have traditionally been divided into two separate methodologies: one for estimating the probability of an accident, and another for assessing its consequences. Limited research has addressed integrating both aspects within a single, unified methodology. Thus, this research aims to advance the research field of probability assessment and to combine this advanced assessment with state-of-the-art ship-bridge consequence assessment into a single maritime risk methodology.

1.2 Aim and objectives

The aim of this thesis is to contribute to the field of maritime risk analysis with a new methodology for assessing the risk of ship-bridge allisions. This aim is motivated by the large investments which bridge construction and maintenance entail, as well as the need to assess more complex risks. Three objectives for this research were formulated:

(i) Develop methods which can quantify different types of ship failure events in terms both frequency and duration.
(ii) Propose a methodology which uses ship failure events in a maritime probability assessment context.
(iii) Combine the probabilistic methodology with a consequence model to assess the risk of allisions.

1.3 Limitations

The methodology presented in the thesis is restricted to the simulation of one ship at a time. This is a distinction and a limitation compared to other maritime risk models, which include ship-ship collision models.

The methodology developed in this thesis utilises existing nonlinear FEA models. The aim is not to advance this type of analysis: instead, the main contribution is the integration of consequence and probability modelling into a single risk methodology. However, consequence is only addressed from a structural point of view; socioeconomic consequences and loss of lives are not evaluated in the proposed methodology.

The methodology proposed in this thesis has been developed for maritime navigation. With some modifications (related to the autopilot and the event modelling), the proposed methodology is likely to work for inland waterways. However, in such cases, other types of failure would be important to consider, such as tight navigations and meeting/overtaking possibilities, which are not covered in this thesis.

Emergency anchoring has not been analysed directly, and the proposed methodology does not include this as a risk control option. However, in areas where it is possible to anchor, the failure durations are shorter, and it is therefore indirectly included.

1.4 Outline of the thesis

The structure of the thesis is as follows: Chapter 2 presents an overview of the existing methods for estimating the risk of allisions. Chapter 3 presents the developed methodology to determine the risk of ship-bridge allision. Chapter 4 presents a brief summary of the case studies in the included papers with which the proposed methodology has been developed. The conclusions are presented in Chapter 5, followed by suggestions for future work in Chapter 6.

2 Review of risk analysis methods connected to ship-bridge allisions

This chapter presents an overview of existing methods used to estimate the risks of ship allisions. The primary focus is previous research on the probability of ship allisions; in addition, a holistic overview of selected state-of-the-art approaches for the consequences of allisions is provided.

Čorić et al. (2021), Galić et al. (2022), and Xiao et al. (2022) conducted reviews on maritime risk models and concluded that most are based on Eq. (2.1), originally proposed by Fujii and Shiobara (1971) and Macduff (1974):

$$N_{\mathrm{a}} = N_{\mathrm{G}} \times P_{\mathrm{C}} \tag{2.1}$$

where N_a is the expected number of accidents, N_G is the number of candidates, and P_C is the causation probability (also referred to as the "aberrancy rate" in some models). Since the introduction of Eq. (2.1), several extensions and refinements have been proposed in risk models published at International Association for Bridge and Structural Engineering (IABSE) conferences (Fujii, 1983; Laheld, 1983; Larsen, 1983; Pyman et al., 1983).

In the 1990s, two major design codes were introduced: the Eurocode and the American Association of State Highway and Transportation Officials (AASHTO). These codes are discussed in Section 2.1. Thereafter, Section 2.2 provides an overview of previous methods used to quantify accident statistics; Section 2.3 presents methods using geometrical models to estimate allision probabilities; and Section 2.4 discusses simulation-based approaches are discussed. Finally, Section 2.5 presents a brief overview of selected methods for maritime allision consequence assessment.

2.1 Bridge building codes and calculation of probability of allision

Building codes exist to ensure that bridges are designed appropriately. The Eurocode (CEN, 2006) and the AASHTO (AASHTO, 2009) both define building codes which are applied in bridge construction, and both include equations for assessing accidental loads resulting from ship-bridge allisions. The Eurocode defines the building standards of bridge construction for European countries, while AASHTO (2009) is not only applied to all bridges in the United States but also used in other parts of the world. The overarching equation is presented in Eq. (2.2), although the codes include additional details and supporting equations:

$$AF = N_{\mathrm{r,sc}} \times PA \times PG \times PC \times PF \tag{2.2}$$

where AF is equal to the annual frequency of bridge collapse, $N_{r,sc}$ is the number of vessels on the route classified into different categories, PA is the probability of vessel aberrancy, PG is the geometric probability (for which it is recommended to use the length of the largest ship as the standard deviation in a normal distribution), PC is the probability of collapse due to a bridge allision, and PF is an adjustment factor accounting for potential mitigation measures included in the fairway design.

Similar to AASHTO, the Eurocode proposes Eq. (2.3) for estimating the probability that a ship will cause a bridge to collapse (CEN, 2006):

$$P_{\mathrm{f}}(T) \;=\; N_{\mathrm{r,sc}} \times fp \times T(1 - p_{\mathrm{a}}) \int_{0}^{\infty} P\{F_{\mathrm{dyn}}(z) > R\} \mathrm{d}z \tag{2.3}$$

where $P_{\mathrm{f}}(T)$ is the probability of bridge collapse during the reference period T, $N_{\mathrm{r,sc}}$ is the annual traffic intensity on route r for ship category sc, fp is the failure probability per unit of travel distance, p_{a} is a factor representing human intervention, z is the position where the failure may occur (and is integrated over the area in front of the bridge), F_{dyn} is the dynamic impact force from the allision, and R is the structural resistance. Although these codes contain slightly different elements, they can be regarded as extensions of the basic Eq. (2.1).

These codes are widely used in engineering practice, though less so in academic research. Two examples of the latter are found in Guo et al. (2022) and Pan et al. (2024), who applied the AASHTO model to estimate the probability of ship allisions; they proposed using the actual distribution of passing ships, derived from AIS data, rather than relying on the length of the largest ship as the standard deviation of the distribution for the geometrical candidates. Additionally, Guo et al. (2022), who studied the Zhoushan-Daishan Cross-Sea Bridge in the East China Sea, emphasised the importance of including the effects of wind and current in areas where these have a significant influence on the navigation. Pan et al. (2024) highlighted another limitation with the Eurocode and the AASHTO: they were primarily developed for inland waterways with narrow navigational channels. Thus, limited information and guidance exist on how to apply them to bridges spanning open waters, and particularly to structures under which multiple ship categories pass.

In addition to these studies, Braestrup (2012) used the Eurocode to estimate the design criteria for the existing Öresund Bridge between Sweden and Denmark; he concluded that more cost-effective designs can be achieved through tailored risk analyses and that the Eurocode was too general.

2.2 Methods to identify failures and derive accident statistics

Galić (2022) reviewed risk models used in academic research and found that many models build on the work of Pedersen (1995), who studied the risks of grounding, allision, and collision. One of Pedersen's (1995) aims was to define the number of accident candidates, N_a, in Eq. (2.1). He concluded that accidents could be categorised into four distinct categories:

(i) The ship follows the intended route, but with too large an offset from the route centre.
(ii) The ship fails to turn at a turning point.
(iii) The ship performs an evasive manoeuvre due to the presence of another vessel and subsequently runs aground or strikes a structure.
(iv) Other types of accidents, such as off-course ships or drifting vessels.

These categories are illustrated in Figure 2-1.

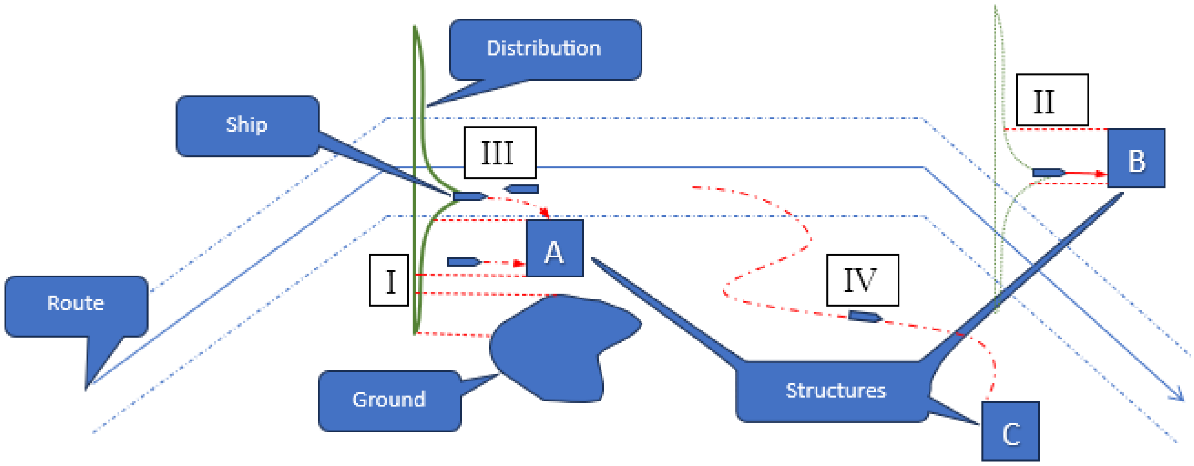

Figure 2-1. The four failure types which cause a ship to strike a structure or run aground, as described by Pedersen (1995). Figure reused from Paper II.

Pedersen (1995) used the fault tree method to derive the causation factor in Eq. (2.1) for failure categories I and II, and he recommended supplementing this method with accident statistics from similar areas to calibrate this factor. However, the probabilities for the remaining categories were not explicitly derived, which Pedersen (2010) highlighted as an area requiring further research. The model was revisited in Pedersen et al. (2020), who suggested using the method proposed by Rasmussen et al. (2012) to obtain these statistics. Rasmussen et al. (2012), for their part, investigated the frequency and duration for accident category II and a subset of category IV accidents—specifically, *loss of propulsion* and *steering machine failure*—using statistics derived from AIS data and Vessel Traffic Service (VTS) reports. Few analyses with a similar aim to Rasmussen et al. (2012) have been found in the literature.

Models building on Eq. (2.1), such as Pedersen's model, rely on causation factors. A comprehensive summary of causation factors from various global locations is provided in the theory guide for the software IWRAP Mk II by Friis-Hansen (2008), with most of these factors found using local accident statistics. Since then, few similar datasets have been published, with notable exceptions including Rasmussen et al. (2012) and Sánchez-Beaskoetxea et al. (2021).

Rasmussen et al. (2012) studied accidents around the Fehmarn Belt between Denmark and Germany, while Sánchez-Beaskoetxea et al. (2021) analysed the occurrence of accidents in the United States related to human error in 1975–2017 and concluded that *lack of trip planning or manoeuvre planning* was the root cause of 18% of all cargo and passenger ship accidents. Other studies by Antão et al. (2023) and Dugan and Utne (2023) examined accident probabilities using global accident databases containing fleet data, and these studies concluded that human error is the most frequent cause of maritime accidents. However, the failure statistics were not clearly separated into categories, nor was the failure duration time compiled, both of which make it difficult to use these statistics in ship-bridge allision analysis.

Closely related to this research on failure statistics and causation factors is the research area of real-time anomaly detection in maritime navigation. On this point, Laxhammar (2008) applied a combination of multivariate Gaussian mixture models and expectation-maximisation algorithms for real-time anomaly detection. More recently, Fan et al. (2024) integrated Kalman filtering into a safety potential field to generate early warnings for inland waterways. Other approaches have combined machine learning techniques with historical accident data to estimate accident probabilities (Fan and Yang, 2024; Gan et al., 2025; Kretschmann, 2020; Munim et al., 2024; Zhang et al., 2025). Rather than relying on historical accidents, Rong et al. (2024) used group clustering with AIS data to detect abnormal behaviour, while Korupoju et al. (2025) applied fuzzy logic to AIS data to estimate ship-ship collision probabilities. Others, such as Gan et al. (2025), have employed neural networks and graph theory to predict future maritime accidents. For their part Xue et al. (2025) used a leaky noisy-max mechanism in a Bayesian model to study ship accidents on the Yangtze River and concluding that enhanced surveillance and monitoring could reduce accident probabilities through more proactive decision-making. Finally, Kowalska and Peel (2012) proposed an active learning model to detect smuggling and terrorism. These types of models are primarily designed to warn an operator of an anomaly, rather than to estimate the frequency of rare events, and they often include false positives; nevertheless, these examples demonstrate the potential of large datasets and advanced analytics to support the development of improved methods for deriving failure statistics.

2.3 Statistical models used to estimate maritime accident probability

One software tool which builds extensively on Pedersen's (1995) equations is the IWRAP Mk II (Engberg, 2017; Friis-Hansen, 2008). This software was developed in cooperation with the International Association of Marine Aids to Navigation and Lighthouse Authorities (IALA), and its use is recommended by the International Maritime Organization (IMO) for quantitative risk assessments (IMO, 2010). IWRAP Mk II was originally designed to assess the probability of collisions and groundings; in later versions, the allision probability was added, using the same equations as those applied to groundings. The software has been applied in several studies; for example, Cucinotta et al. (2017) used IWRAP Mk II to compare the effect of implementing versus not implementing VTS, and Ylitalo (2010) applied IWRAP Mk II to assess accident risks in the Gulf of Finland. Both studies concluded that the software produced results consistent with historical accident statistics; however, Ylitalo (2010) also noted that the results were sensitive to the causation parameters, to how the user defined route layout, and to the parameter for *mean time between checks*.

Hörteborn (2024) conducted a comprehensive comparison between IWRAP Mk II and the Open Maritime Risk Analysis Tool (OMRAT), an open-source implementation (Hörteborn, 2025) of the equations presented by Friis-Hansen (2008). The study investigated the sensitivity of various parameters and confirmed that the same equations used to estimate grounding probability were applied to estimate allision probability. The study concluded that different parameters had varying impacts on accident probability, depending on the model layout; therefore, it is not possible to state that one parameter is always most important to consider in IWRAP Mk II.

Another software tool used to estimate maritime accident probabilities is SAMSON, developed by the company MARINE (Kulendorf et al., 2019). Although designed for use in the North Sea, SAMSON has also been adopted by the Canadian Coast Guard. A key difference between IWRAP Mk II and SAMSON is that the latter includes a small heading deviation in the *miss of turning point* accident type. In a recent comparison study, the probabilities of ship-ship collisions and ship allisions with offshore wind farms in the North Sea were analysed using both SAMSON and IWRAP Mk II in one analysis (ABL and MARINE, 2024). The results showed that both tools produced similar estimates, and while some collision types yielded slightly higher probabilities in IWRAP Mk II, others were higher in SAMSON.

COWI (2008) proposed two models for estimating grounding probability in the Bornholmsgat: one for missed turns, and another for imprecise navigation. The missed-turn model is similar to that proposed by Friis-Hansen (2008), with the addition of a risk reduction factor, k_{RR}. To estimate the probability of grounding, P_x, due to imprecise navigation, COWI introduced Eq. (2.4):

$$P_x = N_g \times \left(D_G(\delta_1) - D_G(\delta_2)\right) \times P_C \times k_{DC} \times k_{RR} \tag{2.4}$$

where N_g represents the annual number of vessel passages; δ_1 and δ_2 denote the lower and upper bounds, respectively, of critical approach angles which could result in a grounding; D_G is the geometrical distribution of vessel courses; and P_C is the causation factor. The factor k_{DC} is a distance compensation factor which accounts for the broader spread of D_G at greater distances from the ground or structures compared to the narrower spread of D_G closer to the ground or structure.

2.4 Simulation models

A variety of computer simulation models have been used to assess accident probability in the maritime domain for decades. This section briefly describes the three categories of models which are most relevant to the proposed methodology: Maritime Transportation System (MTS) models, Maritime Autonomous Surface Ship (MASS) simulators, and Maritime Manoeuvring Simulators (MMS).

MTS models simulate ships' spatiotemporal positions using a simplified time-domain simulation without hydrodynamic effects, where vessels are moved based on a set speed and set course. A few variations of this model have been outlined. Ulusçu et al. (2009) used an MTS model to assess accident risks in the Strait of Istanbul. For this, traffic behaviour was obtained from the VTS data, local operators' websites, and hydrological institutes, and they analysed risks of collision, grounding, ramming, sinking, and fire/explosion. The simulation was repeated 25 times to capture rare events, which were absent in some of iterations. Van Dorp and Merrick (2011) applied an MTS model to coastal areas on the west coast of the USA. In their work, ship routes were based on AIS data, and failure scenarios were based on expert judgement. The study performed a comparison of different scenarios and revealed that the model was not designed to produce absolute values, due to model simplification. Goerlandt and Kujala (2011) developed a similar approach using a dynamic maritime traffic simulator (DMTS), which also relied on AIS data and causation factors for the failure modelling. The DMTS used Monte Carlo simulation methods to simulate meeting situations and to estimate the probabilities of collision and grounding. Rasmussen et al. (2012) used the software ShipRisk to quantify the probability for the Fehmarnbelt Fixed Link project. This internal software was developed by Rambøll and appears to combine Pedersen's (1995) model with MTS-style simulation. All these MTS models omit hydrodynamic forces, making them computationally efficient while simulating ships without failures; however, they are not suitable to analyse ships with failures where the environment dictates the ship movement.

To support MASS voyage planning, more complex simulations are required than MTS simulations. To this end, MASS simulators incorporate hydrodynamic forces in three degrees of freedom (DOF). Xue et al. (2011) used a three-DOF simulator (surge, sway, and yaw) with a potential field method for automatic collision avoidance and autonomous route planning. Although oscillations occurred in tight situations, the model was deemed suitable for autonomous navigation; nevertheless, the authors concluded that it lacked the experience and knowledge of human mariners, and much work was still required before it would resemble human navigation. Wind and current effects were absent in the model proposed by Xue et al. (2011), but these were later included by Johansen et al. (2016), who demonstrated that control behaviours could be tuned for a wide range of scenarios. Shen et al. (2019) implemented a deep Q-learning model for automatic collision avoidance in multi-ship scenarios; in addition to the simulations, they validated their Q-learning model using three self-propelled ships in a test basin. The results were consistent across both environments, and the authors suggested that it was sufficient to test future mathematical models in the simulator. The MASS research field has expanded rapidly in the past decade, with numerous studies proposing different approaches to solving collision avoidance (Liu et al., 2022; Ugurlu and Cicek, 2022; Wang et al., 2024a). The models developed for MASS simulation could be suitable for analysing the allision probability; however, limited research has been found where the MASS suffered from any failure during the simulation.

MMS are widely used for the training of maritime officers, particularly in confined waters and ports where manoeuvring is complex. These simulators prioritise accurate hydrodynamic modelling in four to six DOF, to replicate realistic ship behaviour. MMS are also used in risk assessments for port and fairway design, aiding in defining operational limits (e.g., number of tugboats required for birthing under various weather conditions) (Chen et al., 2018). Weber et al. (2019) used the web-based version of the simulator Seaman Online™ (RISE, 2025) and found it to be an effective tool for teaching ship behaviour in diverse sea conditions. Several major manufacturers—including Transas (now Wärtsilä), Kongsberg, and Rheinmetall—participated in the European Maritime Simulator Network (EMSN) (Poschmann and Wilko, 2017). In addition to accurate modelling of hydrodynamic properties, MMS also offer the possibility to visualise allision scenarios in a 3D environment.

In summary, the different models serve different purposes. The lowest-fidelity simulation models in this review (MTS and DMTS) include various failure types, but the implementation details, frequency, and durations of these failures are often unclear; while these models are fast to run, they cannot simulate ship manoeuvring during turns or speed changes, due to the absence of hydrodynamic calculations. MASS simulators incorporate more advanced hydrodynamic models but are not typically designed to simulate the failure modes experienced by conventional ships. Full-mission MMS offer high-fidelity modelling, including hydrodynamic and failure modes. However, as noted by Chen et al. (2018), MMS are costly to rent and time-consuming to operate, as they often require real-time simulation; both drawbacks have traditionally limited their scalability to scenarios which require thousands or millions of runs. Combining the fast simulations for MASS simulators and MTS models with the capabilities of an MMS is an interesting path with which to analyse the probability of allisions.

2.5 Consequence models

One of the pioneers in the domain of consequence assessment of ship-structure allision was Minorsky (1958), who studied ship-ship collisions to establish safety standards for protecting nuclear power plants. Based on accident reports from the coast guard, he found that the volume of deformation in the ships involved in a collision was related to their kinetic energy. Since then, numerous analytical and semi-analytical methods for analysing structural integrity and crashworthiness consequences have been developed based on Minorsky's work. Most recent studies use nonlinear FEA to model the complex hydro-mechanical coupling effects. Typically, consequence modelling in collisions and allisions consists of two major components: external dynamics and internal mechanics. For the latter, Haris (2013) proposed dividing the study of internal mechanics into three categories:

- **Experimental studies,** where physical tests are used to develop several simplified models which align with the empirical results. For examples, Amdahl (1983) conducted a few full-scale measurements to understand the energy absorption in oil platforms, and Tabri et al. (2008) performed model tests of ship-ship collisions.

- **Simplified analytical models,** which are generally fast and cost-effective, making them suitable for risk analysis. These models were first introduced by Minorsky (1958) and further developed by Zhang et al. (2017) and Pedersen et al. (2020). Energy dissipation is estimated based on the volume of damaged material in the ship's bow structure.
- **Numerical simulations,** which typically use FEA solvers such as ABAQUS (Abaqus, 2023) and LS-DYNA (Ansys, 2024).

Pedersen's extensive research over the last half century (Petersen and Pedersen, 1981; Pedersen and Jensen, 1991; Pedersen et al., 1993; Pedersen, 1995; Pedersen and Zhang, 1998; Pedersen et al., 2020) has demonstrated the feasibility of combining analytical, semi-analytical, and FEA methods in ship collision and allision analyses. Some of these studies have also shown that simplified analytical expressions can effectively represent internal energy dissipation during ship-ship collision events. Furthermore, Zhang et al. (2017) compared physical trials with Pedersen's equations and found strong agreement between the theory and the physical tests.

Understanding how two bodies crash and deform is a key topic across disciplines. Le Sourne et al. (2012) described how Mitsubishi developed a collision module (named MCOL) within in the FEA solver LS-DYNA to model both internal mechanics and external dynamics. Le Sourne et al. (2012) extended this to maritime applications by developing the software SHARP, which enables detailed assessments of structural integrity consequences in consideration of hydrodynamic-mechanical couplings. In connection with the Norwegian E39 fjord crossing project, consequences of ship-bridge allisions have been studied extensively (Sha et al., 2021, 2019a, 2019b; Sha and Amdahl, 2019; Wang et al., 2023). Sha et al. (2019a) simulated local structural damage using LS-DYNA and combined global dynamic bridge responses using USFOS software (Søreide et al., 1993). Wang et al. (2023) continued this research using OrcaFlex software (Orcina, 2022) to analyse ship-bridge allisions under wind and wave conditions; their study concluded that while wind and wave loads significantly affect the structural integrity in an allision, the location and the angle of attack have an even greater effect on the result.

Combining internal mechanics with external dynamics is often referred to as coupled simulation. As illustrated by Márquez et al. (2022), ship hydrodynamics have a major influence on the forces in ship-ship collisions. Internal mechanics require detailed modelling of the impact area, while external dynamics require simulation of the entire vessel. Varying mesh sizes can be used in coupled simulations, to reduce computational demands (Rudan et al., 2019). Although most examples in the literature have focused on ship-ship collisions, coupled simulations have also been applied to analyse the consequences of ship-floating offshore wind turbine allisions (Ladeira et al., 2023; Márquez et al., 2022; Ren et al., 2022) and ship-bridge allisions (Sha et al., 2021, 2019a, 2019b, 2019c; Sha and Amdahl, 2019). These combined simulations seem to be state-of-the-art and thus suitable for use in the consequence assessment of ship-bridge allisions. Specifically, Larsen (1993) illustrated how the force decreases with the height of the impact area, as it requires less force per meter to deform the top floor than the ship deck; therefore, it is important to distinguish between the probabilities of ship-girder (bridge deck) allisions and ship-pontoon allisions. Sha and Amdahl (2019) studied ship-girder allisions and came to the same conclusion as Larsen (1993), namely that the upper decks of the ship superstructures are generally weaker than the lower decks and the bridge girder. However, as regards ship-girder allisions, which structure (i.e., the bridge or the ship superstructure) is deformed depends most on the material and the design of both the bridge and the ship. A real-world example is the ship KAREN DANIELSEN, who struck the west part of the Great Belt Bridge in 2005 and completely tore off the ship superstructure (BMA and DDIMA, 2005).

Finally, a sensitive aspect of FEA simulations is user assumptions. Ringsberg et al. (2018) conducted a benchmark study involving 15 experienced research groups and the simulation of an indenter impact experiment on a ship-side shell structure. The study revealed some scatter in the results regardless of whether ABAQUS or LS-DYNA was used, which highlights the influence of user assumptions. Chen et al. (2024) reached a similar conclusion when comparing different FEA methodologies. Furthermore, it is important to note that factors such as impact angle, material degradation, ship speed, and ship design significantly affect the amount of energy transferred to the structure during an allision; therefore, a holistic approach to conducting risk assessments may be more appropriate for the consequence assessment. In addition, it would be valuable to examine whether integrating several detailed consequence assessments could serve as a robust approach for approximating outcomes across a range of allision scenarios. By compiling results from diverse case studies, it may be possible to capture a broader variability and to improve the accuracy of consequence predictions. Such an approach could enhance risk assessments and create both a more resilient design and better mitigation strategies.

3 Methodology

The proposed methodology is labelled as Ship Traffic Allision Probability using Monte Carlo Simulations – consequence (STAPS-cons). The basic idea of this methodology is the running of manoeuvring simulations of failure events for ships in “fast-time mode” to determine the risk of ship allision. However, before any simulations are conducted, it is important to understand why these failure events occur; therefore, capturing local ship failure statistics is an important step of the methodology. STAPS-cons can be divided in four steps, illustrated in Figure 3-1.

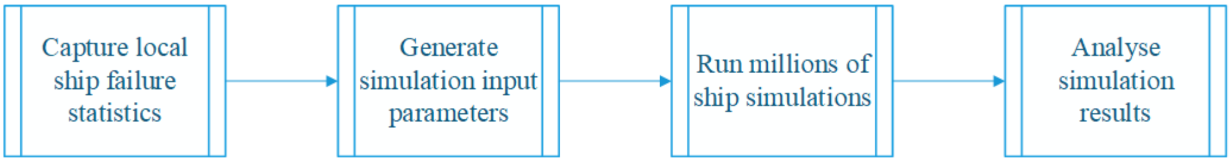

Figure 3-1. Overview of the methodology steps in STAPS-cons.

The methodology has been developed in the studies outlined in the four appended papers. Papers I, II, and III primarily focus on the probability of an accident and the development of STAPS; Papers I and III also demonstrate the possibility to quantify mitigation actions with the methodology. In Paper IV, the methodology is extended to also include the consequences of an allision; this extended version of the methodology is referred to as STAPS-cons. Figure 3-2 highlights some keywords from each paper and the connections between the papers.

	Paper I A method for risk analysis of ship collisions with stationary infrastructure using AIS data and a ship manoeuvring simulator	Paper II Probability of active navigational failures - Incident analyses for use in ship-bridge allision risk assessments	Paper III Probabilistic analysis of ship-bridge allisions when designing bridges	Paper IV Risk analysis methodology for ship-bridge allisions – A combined probability and consequence analysis
Journal	Ocean Engineering	Journal of Navigation	Reliability Engineering & System Safety	Engineering Structures
Aim	Introduce the simulation methodology STAPS	Quantify active navigational errors	Enhance STAPS and compare it with IWRAP Mk II	Include consequence estimations to form STAPS-cons
Case study area	Great Belt Bridge	Different waters in Scandinavia	Halsafjorden Bridge	Bjørnafjorden Bridge

Figure 3-2. Connection between the included papers.

The proposed STAPS-cons methodology, developed across the four appended papers, is described in the upcoming sections of this chapter:

- **Section 3.1** outlines how AIS data have been structured to support the development of the methodology.
- **Section 3.2** explains how AIS data are used to derive failure statistics, which are categorised into two types: passive failures, presented in Paper I; and active navigational failures, presented in Paper II.
- **Section 3.3** describes the transition from historical failure data to the estimation of ship-bridge allision probabilities, which is applied in Papers I, III, and IV.
- **Section 3.4** presents how the consequences of allisions are included in the methodology to form a risk analysis framework, demonstrated in Paper IV.
- **Section 3.5** provides a summary of the data, tools, and models used throughout the thesis, clarifying the distinction between original work and supporting resources.

3.1 The use of AIS data

The foundation of the proposed methodology is good availability of AIS data. Since the introduction of AIS in 2002, all Safety of Life at Sea (SOLAS) ships have been required to transmit AIS messages (IMO, 1998). Ships equipped with an AIS-A transponder transmit two types of AIS messages: a dynamic message and a metadata message. Each ship issues a dynamic message at intervals of 2–10 seconds (depending on the ship's speed and rate of turn) and a static message every 6 minutes (ITU-R, 2014). The dynamic message contains information including the Maritime Mobile Service Identity (MMSI) number, ship position, speed, course, heading, rate of turn, and navigational status; the static message includes information regarding the MMSI number, ship draft, type of ship, estimated time of arrival, destination, IMO number, and antenna position.

In this thesis, AIS dynamic messages have been used both as "single points" and as "trajectories". The latter are obtained by combining multiple single points into trajectories, as illustrated in Figure 3-3 (where 12 fictional AIS position reports are combined into 3 trajectories). Guo et al. (2024) analysed eight different methods for generating trajectories from AIS points and concluded that the top-down kinematic compression method was the most effective; accordingly, a similar approach is used in this thesis. This method of combining messages has several advantages compared to using single points: first, it reduces the volume of data stored in the database; and second, missing data points are less likely to cause inconsistencies with jumping data points, something which Liu et al. (2023) and Yan et al. (2022) have highlighted as an issue with AIS data. The lines in Figure 3-3 represent AIS messages with similar speed over ground (SOG) and course over ground (COG); in the figure, the red and blue lines share the same COG but differ in their SOG, while the green line on the right represents messages with both a different COG and SOG from the red.

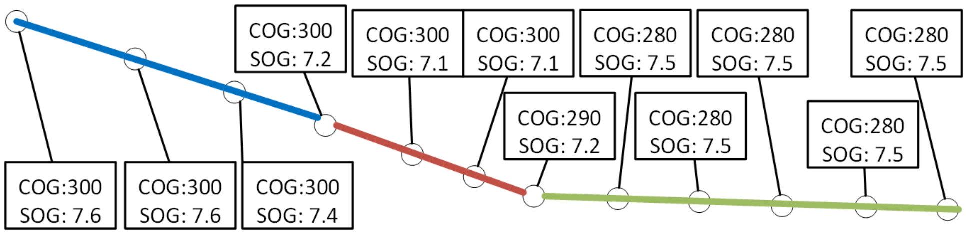

Figure 3-3. Illustration of how AIS position reports are converted to trajectories. Figure reused from Hörteborn (2021).

The AIS data used in this research are continuously streamed from various sources and stored as encoded text, with a timestamp, in text files. The generated AIS trajectories used in the analysis are stored in an in-house PostgreSQL database with the spatial extension PostGIS. Data selection from the database was performed using structured query language (SQL), while data analysis and visualisation were carried out using Python and QGIS.

The advantage of AIS data is that it is continuously broadcasting to any receiver, which enables extensive studies of ship traffic over large areas and long time periods. This represents a major advancement in available data since Fujii and Shiobara (1971) and Macduff (1974) initiated this field of research. AIS data is limited, however, in that it only includes spatiotemporal data: it does not capture onboard machinery status or the verbal communication between ship bridges. Such data are typically recorded, but they are stored locally on the ship in the voyage data recorder.

3.2 Capture of failure statistics

As outlined in Figure 3-1, the first input for the proposed methodology is local failure statistics, collected from AIS data close to the case study area. In the context of this thesis, the term "failure" refers to unintended events experienced by ships; while undesirable, these are frequently resolved before escalating to accidents (such as groundings or allisions). To find these events, trajectories from several years of AIS data are used to filter out and identify "failure candidates". Then, the original single-point data for these candidates are retrieved, and ship contours are added; these contours are then manually analysed spatiotemporally using the QGIS software. Through this combination of trajectory and ship contour analysis, five types of failures have been identified, which were summarised in Paper III as:

1. **Loss of propulsion:** The ship is drifting with the environment, and its propeller(s) is set to 0 rpm. There is a 50/50 chance of continuing use of the rudder(s) to manoeuvre in a limited manner (even if some ships alter their rudder(s) during a loss of propulsion, their efficiency is decreased). Could cause a category IV accident (see Figure 2-1).
2. **Loss of steering:** The ship makes a sharp turn by setting its rudder(s) to full port/starboard and the propellers(s) to 0 rpm. Based on the studied failure, it is assumed to have a faulty control system and reduces its speed. Could cause a category I or IV accident (see Figure 2-1).

3. **Miss of turning point:** The ship continues straight ahead instead of turning where required. This failure type also includes a ship which attempts to find its way back to the normal path. This is similar to accident category II (see Figure 2-1).
4. **Wrong course at a turning point (WCT):** The ship turns at the correct location but sets the wrong course. Could cause a category I or IV accident (see Figure 2-1).
5. **Turn at the wrong location (TWL):** The ship makes an active turn at a location which puts it at risk of an accident. Could cause a category I or IV accident (see Figure 2-1).

While Figure 2-1 describes accident paths as categorised by Pedersen (1995; 2020), Figure 3-4 illustrates failure types which could potentially lead to accidents.

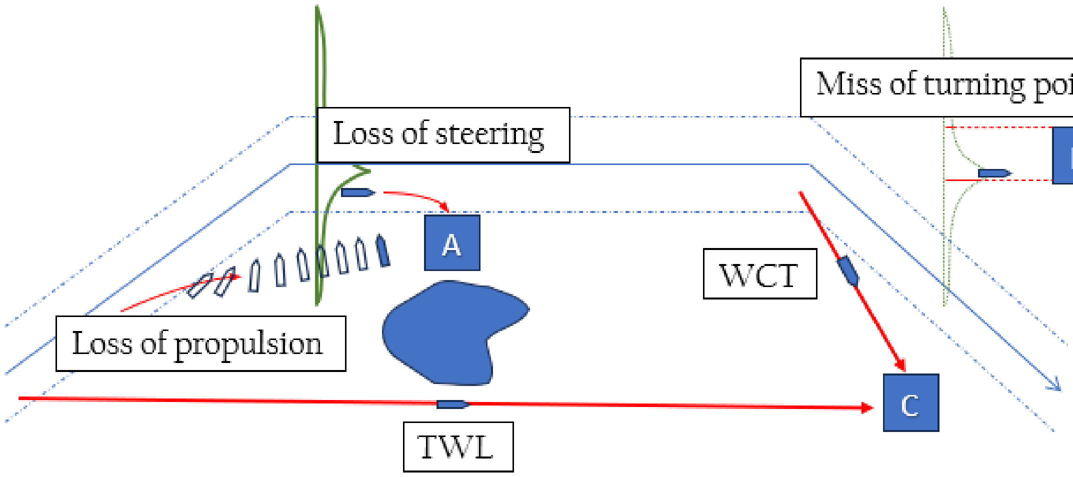

Figure 3-4. Examples of a sailing fairway, passing one island and three structures (A, B, and C). Paths of the five failure types are shown, to illustrate how each could result in an allision. Figure reused from Paper III.

Failure types *loss of propulsion*, *loss of steering*, and *miss of turning point* are considered passive failures and are further described in Paper I; *WCT* and *TWL* are considered active navigational failures and are further described in Paper II. Generally, the failure types *loss of propulsion* and *loss of steering* were identified by comparing the COG and heading of all trajectories in an area; those differing by more than 20 degrees were manually observed. This manual inspection included an extended analysis of the vessel's journey, the prevailing weather conditions, destination, and estimated time of arrival. Most of the identified vessels were engaged in slow steaming or exhibited prolonged low-speed phases, resulting in significant drift angles. However, a subset of cases revealed more distinct failure behaviours, wherein vessels maintained normal speed, experienced temporary drifting, and subsequently resumed typical operation. In a few instances, ships deviated from the fairway and anchored, indicating potential loss of control or navigational anomalies.

The workflow for identifying the failure types *miss of turning point*, *WCT*, and *TWL* are presented in Figure 3-5.

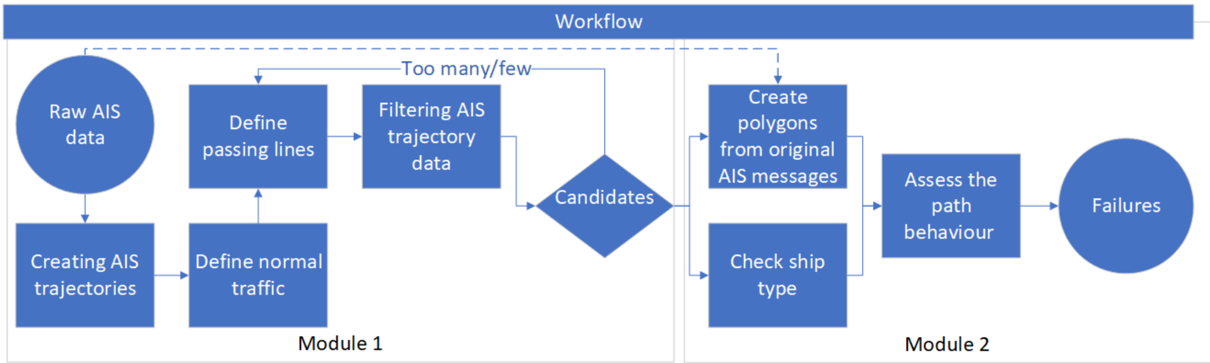

Figure 3-5. Workflow for quantifying the failure types *miss of turning point*, *WCT,* and *TWL*.
Figure reused from Paper II.

In order to determine where to place the passage lines for identifying *WCT* and *TWL* failures, accident and incident reports were analysed to understand how previous cases developed. If these lines are placed too close to the traffic lane centre, too many candidates are identified, making the manual analysis of their behaviour overwhelming; however, if the lines are placed too far off from the centre, too few candidates are identified, and potential failures may be missed. Therefore, an iterative approach to placing these passage lines is important, so as to balance sensitivity and workload. An example of how these passage lines could be drawn is illustrated in Figure 3-6.

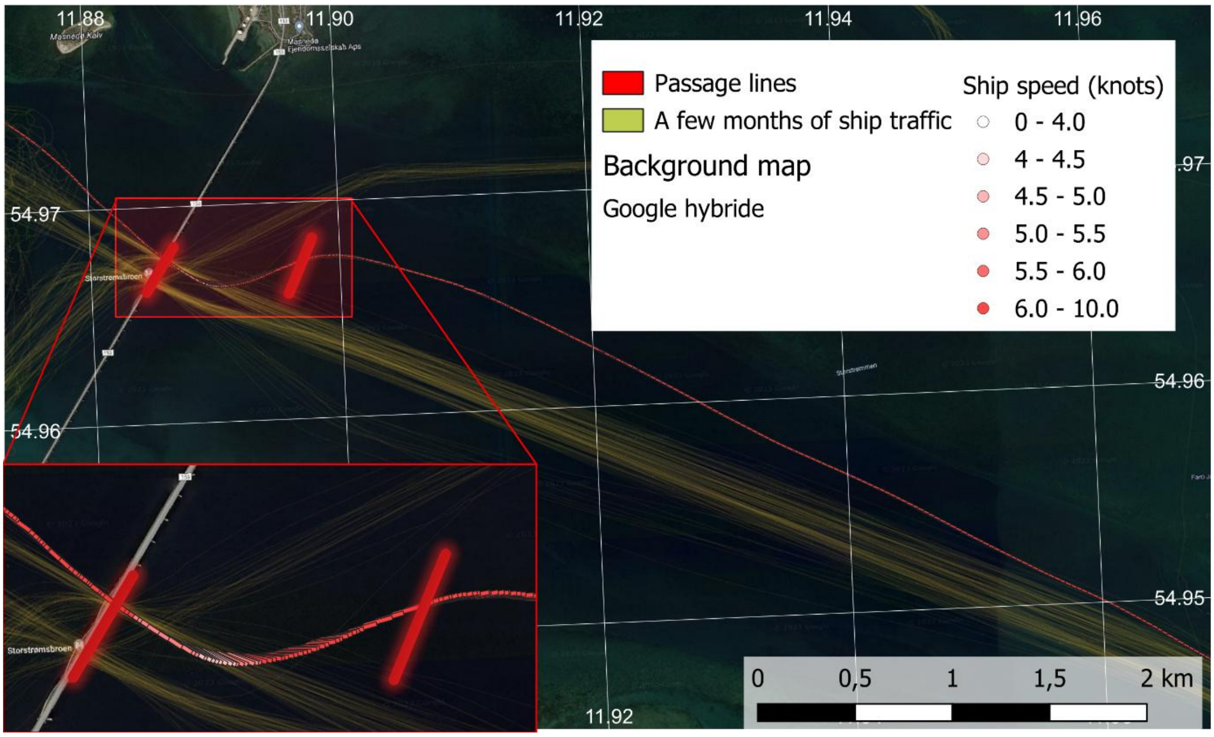

Figure 3-6. Passing lines and one active navigational error for the Storstrømsbron. Figure reused from Paper II.

Failure duration is another important aspect of the STAPS methodology (in Paper III, the terminology "repair time" was also used for failure duration). Durations were measured using the AIS point data from the timestamp prior to the initiation of the failure event to the timestamp when the ship was deemed "under control" (which was defined as either back en route or safely anchored). For the failure types *loss of propulsion*, *loss of steering*, *WCT,* and *TWL*, durations were fitted to a lognormal distribution, while for *miss of turning point*, durations were fitted to a normal distribution.

The overall conclusion is that each geographical area is unique. For example, areas with shallow waters increases the grounding probability, but they also enhance situational awareness and see reduced duration of failures, as the crew is more alert. As a result, both the probabilities and the durations—especially for *miss of turning point* and for active navigational errors—have limited applicability outside the specific areas in which they occurred. This highlights the importance of using location-specific data when conducting risk assessments.

3.3 Capture of probability of ship-bridge allisions

In the research presented in this thesis, the Seaman simulator, a proprietary extension of PYSIM (sspasweden, 2020), is used as an MMS. It utilises the Odeint solver from the Boost library (Ahnert and Mulansky, 2024) to solve hydrodynamic differential equations. The simulations are conducted in the time domain using a fourth-order Runge-Kutta method. Ships are simulated with an autopilot system controlling the rudder and engine to follow a predefined route at the correct speed. Prior to the introduction of any failure, the simulation is run under normal conditions to ensure that the ship can follow the intended route in all-weather conditions. Figure 3-7 illustrates the key concepts and how they are connected in the STAPS-cons methodology.

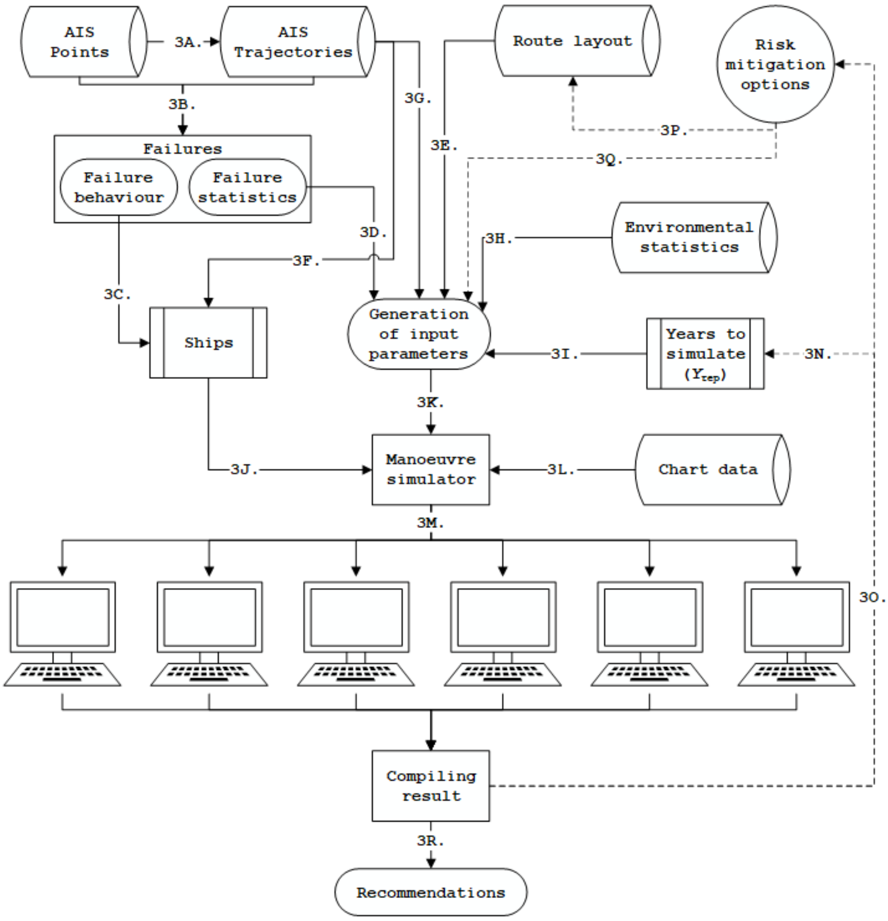

Figure 3-7. A schematic of the simulation methodology in STAPS.

3A. AIS data is generated and transmitted from ships as point data, then translated into trajectories using the method described in Section 3.1.
3B. Both the point data and the trajectories are used to identify and quantify failures, as described in Section 3.2.
3C. The behaviour of ships with failures is implemented in the ship model logic.
3D. The failure frequency and the duration distribution are used to generate input parameters.
3E. The route layout (i.e., coordinates for simulated ships) is drawn by the user.
3F. AIS trajectories are used to obtain normal traffic data, including which ship categories to simulate.
3G. The number of ships, their speeds, and their lateral distribution over the route are determined.
3H. Weather statistics (winds, waves, currents) from the area are included in the generation of input parameters.
3I. The parameter "Years to simulate (Y_{rep})" determines how many repetitions of the traffic should be used in the simulation.
3J. Ship definitions are added.
3K. Input parameters are generated using the Monte Carlo simulation technique, creating millions of variations of start settings to run.
3L. Chart data, including bathymetry and bridge layout, are added.
3M. Simulations are executed for multiple processes.
3N. After simulations are completed, the Y_{rep} parameter is checked with Eq. (3.4).
3O. Different risk mitigation options are evaluated.
3P. Options in 3O could include alterations of the route layout.
3Q. Other options in 3O could also include changes directly influencing the generation of input parameters, such as speed limitations or traffic control.
3R. Recommendations are provided based on the analysis.

The number of simulations to be run depends on several parameters, which are summarised in Eq. (3.1) and detailed in Eq. (3.2) and (3.3). Each combination of ship category (sc), route (r), and failure type (ft) is combined into *sets,* and the number of simulations is estimated using Eq. (3.2) and Eq. (3.3).

$$N^{\mathrm{sim}} = \sum_{\mathrm{sc}}^{\mathrm{no.\ sc}} \sum_{\mathrm{r}}^{\mathrm{no.\ r}} \left(\sum_{\mathrm{ft}}^{1,2,5} N^{\mathrm{sim}}_{\mathrm{ft,sc,r}} + \sum_{\mathrm{ft}}^{3,4} M^{\mathrm{sim}}_{\mathrm{ft,sc,r}} \right) \tag{3.1}$$

The estimation process is divided between two groups: failures initiated prior to a turning point (*miss of turning point* and *WCT*), and other failure types initiated at regular intervals along the route (*loss of propulsion*, *loss of steering*, and *TWL*). For the latter group, where failures are evenly spaced, the number of simulations in each set $N^{\mathrm{sim}}_{\mathrm{ft,sc,r}}$ is estimated by Eq. (3.2):

$$N^{\text{sim}}_{\text{ft,sc,r}} = N_{\text{r,sc}} \times P_{\text{ft}} \times \left(\frac{L_{\text{r}}}{v_{\text{sc}}}\right) \times Y_{\text{rep}} \tag{3.2}$$

where $N_{r,sc}$ is the estimated number of ships on route r in ship category sc, P_{ft} is the failure frequency (expressed in failures per hour; unique for each failure type), and Y_{rep} is the number of repetitions of one year's traffic represented in the simulation. The distance between starting positions along the route is given by N^{sim} divided by the route length L_r.

For failures that occur at planned turning points, the number of simulations $M^{sim}{}_{ft,sc,r}$ is estimated by Eq. (3.3):

$$M^{\text{sim}}_{\text{ft,sc,r}} = N_{\text{r,sc}} \times P_{\text{ft}} \times N_{\text{turns,r}} \times Y_{\text{rep}} \tag{3.3}$$

where $N_{turns,r}$ is the number of turns per route.

Once the number of simulations is determined, large sets of input parameters are generated using a Monte Carlo simulation technique. Each simulation receives a unique set of input parameters based on their respective distributions in the Monte Carlo simulation; these parameters are then used by the simulator's autopilot to control the ship during the simulation. The simulation is terminated when the failure duration runs out or the ship runs aground or strikes a structure. A 15-minute voyage takes less than a second to complete in "fast-time mode" and voyages can be run in parallel, enabling millions of simulations to be completed within a few hours. All data for involved ships are stored and can be analysed further.

Still, the generation of input parameters in the Monte Carlo simulation method introduces randomness into the results. To mitigate this, the value of Y_{rep} in Equations (3.2) and (3.3) can be increased. A threshold is defined to determine an adequate Y_{rep}, such that the spread in the "expected number of allisions during the design period", A, should be less than 5% based on three realisations (i) of the input parameters, as expressed in Eq. (3.4).

$$0.95 \leq \frac{A_{\text{i}}}{\frac{A_1 + A_2 + A_3}{3}} \leq 1.05 \text{ for i } \in \{1,2,3\} \tag{3.4}$$

A maximum of 5% difference between three seeds was found to be a good balance between number of simulations and accuracy. To ensure that these realisations of parameters are both random and repeatable, a NumPy RandomState object was utilised; Harris et al. (2020) explained that this object guarantees that fixating the seed will return the same pseudorandom values from a wide range of distributions.

3.4 Capture of consequence analysis of ship-bridge allisions

The consequences of a ship-bridge allision can be quantified in different measures, such as the amount of energy transferred in the allision, the lives lost, or the rebuilding cost. These quantities are all important to consider; however, the focus in this thesis is on energy. In Paper

I, only the kinetic energy of the ship prior to impact is considered. In Paper IV, the consequence analysis is extended to also include the allision and how energy is transferred from the striking ship's initial kinetic energy. The initial kinetic energy is simplified in Eq. (3.5):

$$K = \frac{(D_{sc} + A11_{sc}) \times u^2}{2} + \frac{(D_{sc} + A22_{sc}) \times v^2}{2} \tag{3.5}$$

where D_{sc} is the displacement of the ship, u is the forward speed, v is the lateral speed, $A11_{sc}$ is the added mass in longitudinal direction, and $A22_{sc}$ is the added mass in the lateral direction.

The worst allision simulated in Paper I—i.e., the one with the highest kinetic energy—is assumed to occur once every Y_{rep} years, and the second worst (or worse) is assumed to occur twice within Y_{rep} years. Based on this logic, the worst allision can be determined for any given probability (assuming that Y_{rep} is sufficiently large).

The consequence assessment in the STAPS-cons methodology uses multiple models, requiring three different coordinate systems. The simulator uses a global coordinate system (X, Y). For pontoon allisions, a coordinate system aligned with pontoon orientation (rotated by γ_1, relative to the X, Y coordinate system) is used. Finally, to distinguish between sliding and head-on allisions, a third coordinate system aligned with impact surface (rotated γ_2, relative to the surface coordinate system) is used. These systems and the angles β and α are illustrated in Figure 3-8.

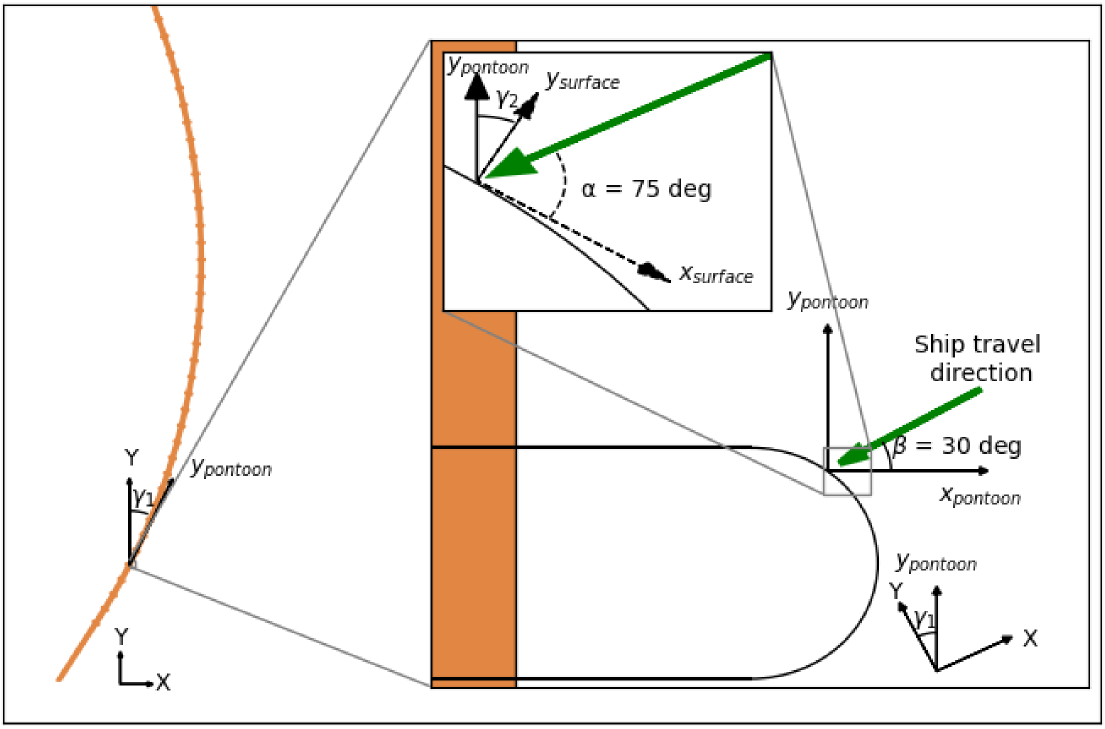

Figure 3-8. The three coordinate systems used in STAPS-cons. The green arrow indicates the ship's direction. (X, Y) is used in the MMS model; ($x_{pontoon}$, $y_{pontoon}$) is used to calculate the β angle for pontoon allisions; ($x_{surface}$, $y_{surface}$) is used to calculate the sliding allision angle. Figure reused from Paper IV.

Following the division in Wang et al. (2024b), the ship's kinetic energy just before it hits a structure K_0 is divided into seven components after the allision, as shown in Eq. (3.6):

$$K_0 = K_{pos,ship} + K_{pos,structure} + W_{hyd,ship} + W_{hyd,structure} + E_{int,ship} + E_{int,structure} + W_{fri} \quad (3.6)$$

where K_{pos} is the remaining kinetic energy in the ship/structure post-allision, W_{hyd} is the work done by the hydrodynamic forces of the ship/structure, E_{int} is the internal structural deformation energy in the ship/structure, and W_{fri} is the work done by friction forces.

In the case of oblique or sliding allisions, the remaining energy in the ship, $K_{pos,ship}$, is estimated using the Eurocode (CEN, 2006), which defines lateral impact angle as those with an angle α (se Figure 3-8) below 45°, given in Eq. (3.7):

$$K_{pos,ship} = \begin{cases} K_0 \times \cos(\alpha), & \alpha < 45 \\ 0, & \alpha \geq 45 \end{cases} \quad (3.7)$$

The remaining energy components in Eq. (3.6) are estimated using nonlinear FEA for a few selected cases; these components are assumed to be directly obtained from the FEA simulations. While this thesis does not include modelling of bridge structures or the execution of FEA simulations itself, it focuses on the integration of results derived from such models. Paper IV uses simulations from Jin et al. (2020), which are based on a decoupled sequential local and global FEA simulation methodology described by Sha et al. (2019a). The model includes all major structural components, including the outer panels, decks, bulkheads, frames, and stiffeners, as illustrated in Figure 3-9.

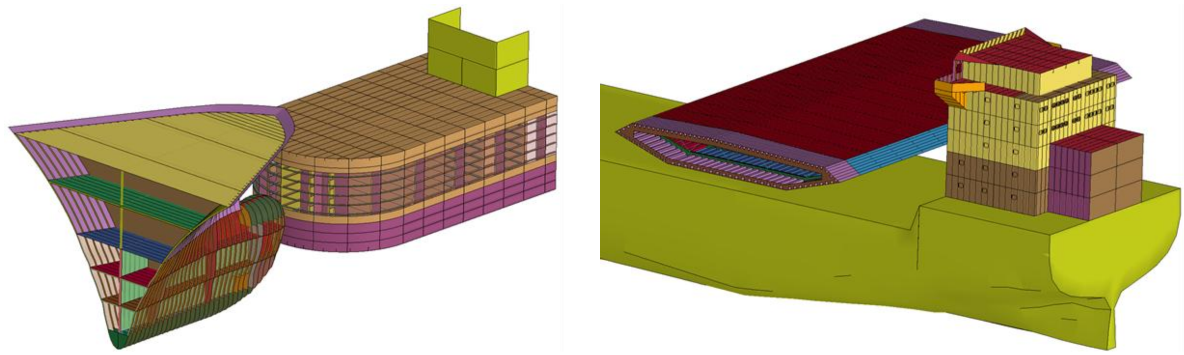

Figure 3-9. (Left) The FE model of the ship and the pontoon, and (right) the FE model of the ship deckhouse and bridge girder. The different colours represent different materials in the FE models. Figure reused from Paper IV.

The internal structural deformation energies ($E_{int,ship}$ and $E_{int,bridge}$), the friction energy (W_{fri}), and a force-deformation curve are calculated in the local FEA simulation; this curve is then used in the global FEA simulation, where the bridge is modelled as a generalised beam to represent its global structural stiffness. The global simulation yields the kinetic energies of the bridge after the allision ($K_{pos,bridge}$) and the hydrodynamic work forces ($W_{hyd,ship}$ and $W_{hyd,bridge}$). In Sha et al. (2019a), the local simulation was also performed before the global simulation, which is justified by the long natural period of the bridge. While including global boundary conditions in the local model would improve accuracy, the added complexity and computational cost are not considered worthwhile. In any case, the STAPS-cons methodology can use results from any FE software and modelling techniques.

Once all terms in Eq. (3.6) are known, an additional matrix of FEA simulations is required to determine the maximum capacity for each structure. This capacity is defined in two parts: a local maximum capacity (C_{l}, in MJ), and a global maximum capacity (C_{g}, in MJ). If either of these capacities are exceeded, the structure is assumed to collapse. The total number of collapses (N_{collapse}) over Y_{rep} years is calculated using Eq. (3.8):

$$N_{\mathrm{collapse}} = \sum_{i=1}^{\text{no. allisions}} \begin{cases} 1 & E_{\mathrm{int,bridge}_i} > C_{\mathrm{l}}\ or\ \left(K_{\mathrm{pos,bridge}_i} + W_{\mathrm{hyd,bridge}_i}\right) > C_{\mathrm{g}} \\ 0 & Otherwise \end{cases} \tag{3.8}$$

The ability to analyse allision risk against a bridge design criterion is a central feature of the proposed methodology. According to the Norwegian national annex to the Eurocode (which has no equivalent in the Swedish or Danish annexes):

> *"The occurrence and consequence of accidental loads are usually related to a specific risk level. To the extent that the accidental load can be determined using probability calculations, the probability of events that are disregarded in the analysis should not exceed 10^{-4} per year."* (Statens Vegvesen, 2014, p. 75).

This implies that a bridge must withstand all allisions with a probability of occurrence greater than once every 10,000 years. By identifying the 100th worst allision in a simulation with Y_{rep} set to 10^6, the STAPS-cons methodology can be used to determine this design threshold. Furthermore, together with the design criterion, the expected number of structural collapses can help structural engineers define C_{l} and C_{g} for the structure. This design criterion could also be used in sensitivity analyses to examine how input parameters affecting both the probability and consequence assessments could be analysed.

3.5 Overview of data, methods, and uncertainties

Although the methodology has been described throughout this chapter, an overview is provided here to clarify the technical components used and to distinguish between original contributions and supporting resources.

The core methodological development in this thesis is the STAPS-cons framework, which combines probabilistic modelling, failure statistics, and consequence analysis into a unified approach for assessing ship-bridge allision risk. This framework was designed, implemented, and validated as part of the research presented in Papers I–IV.

AIS data were primarily acquired from the Swedish Maritime Administration and the Norwegian Coastal Administration. The data are stored incessantly at RISE, and records from 2006–2024 have been used in this research. The data were processed using scripts developed in-house to unpack and load trajectories into a PostgreSQL database with the PostGIS extension. Custom scripts were also developed to filter trajectories, identify failure events, and classify the latter into five distinct types. The statistical treatment of failure frequency and duration was developed within the scope of this work, combining automated processing with manual inspection.

Ship manoeuvring simulations were carried out using Seaman's 2D time-domain simulator. While the simulator itself has been developed over several decades at SSPA and RISE, all simulation scenarios, parameter selections, and result interpretations were designed and executed within the scope of this research. The simulator was operated in fast-time mode to enable large-scale Monte Carlo simulations, which were essential for estimating the accident probabilities.

Consequence modelling was supported by pre-existing nonlinear FEA of ship-bridge allisions. Although the FEA simulations were not performed as part of this work, results from previous studies were integrated into the STAPS-cons framework; this included the use of energy-based collapse thresholds and probabilistic consequence modelling, which were adapted and applied to support the overall risk estimation.

The use of multiple input sources in this methodology entails uncertainties. Uncertainty related to the number of ships en route has a linear correlation with the probability of allision. The layout of the area (including structures and routes) has a major impact on how much influence the remaining input parameters have on the allision probability. A simple example is layouts without any routes pointing towards a structure; in such cases, the allision probability is unaffected by changes in the frequency and duration of the failure types *miss of turning point* and *WCT* (and the uncertainty in these parameters). For other layouts, uncertainty in these parameters may have a major influence on the allision probability. The failure frequency has a linear correlation with the number of failures caused by that failure type; however, the duration of failure has a more complex correlation with the allision probability, and the uncertainty of this parameter should be carefully investigated for each layout. Furthermore, there may be considerable uncertainty regarding how future ship traffic will pass a structure. With respect to the consequences of an allision, uncertainty in ship displacement has a linear influence on kinetic energy, while uncertainty in ship speed (drifting or powered) has a quadratic influence. Additionally, uncertainties in ship design and material degradation may also influence the probability of collapse.

This overview clarifies the methodological boundaries between original work and external tools and data sources. The integration of these components into a novel and operational risk assessment framework represents a central contribution of the thesis. Compared to other frameworks, STAPS-cons has reduced uncertainty related to hydrodynamic effects, impact location, and impact direction.

4 Summary of appended papers

The failure statistics are a key part of this research; therefore, they are the specific focus of the first section of this chapter (Section 4.1), which looks at the failure statistics from each of the four appended papers. This is followed by four sections, each presenting a summary of a paper and a brief presentation of the case studies analysed in that paper.

4.1 Summary of the failure statistics obtained

In Paper I, 153 passive failures were identified in the Great Belt VTS and the TSS Bornholmsgat, utilising the method described in Section 3.2. The same methodology was used in Paper III, which identified 61 passive failures in the area surrounding Halsafjorden. Active navigational failures were only studied in Paper II; here, 17 failures were identified based on AIS data, another 15 were identified from incident reports, and 11 failure tracks were found in accident reports.

The frequencies of the failure types *loss of propulsion, loss of steering*, and *TWL* were calculated by dividing the number of events by the number of sailing hours, while the frequencies of the failures *miss of turning point* and *WCT* were calculated by dividing the number of failures by the number of ships making the assessed turn. The frequencies of the passive failure types, along with the Danish data in Rasmussen et al. (2012), are presented in Table 4-1, and the frequencies from the active navigational errors are presented in Table 4-2.

Table 4-1. Summary of the frequencies of passive failures, together with the frequencies in a case study presented in Rasmussen et al. (2012).

Failure category	Great Belt VTS	TSS Bornholmsgat	Halsafjorden	Rasmussen et al. (2012)
Loss of propulsion	0.65×10^{-4}/hour	0.91×10^{-4}/hour	1.17×10^{-4}/hour	1.5×10^{-4}/hour
Loss of steering	0.038×10^{-4}/hour	0.092×10^{-4}/hour	0.21×10^{-4}/hour	0.63×10^{-4}/hour
Miss of turning point	1.55×10^{-4}/turn	2.10×10^{-4}/turn	-	2.5×10^{-4}/hour

Table 4-2. Summary of the frequencies of active failures.

Failure category	Scandinavian bridges	Halsafjorden
WCT	0.69×10^{-4}/turn	1.3×10^{-4}/turn
TWL	16×10^{-4}/turn	-

The failure probabilities found for Halsafjorden are closer to the probabilities found in Rasmussen et al. (2012) but relatively high compared to the other locations. Sufficient cases to determine statistics for *miss of turning point* and *TWL* failures were not found for Halsafjorden. The tables show some interesting similarities; for example, *loss of propulsion* is more frequent than *loss of steering.* Furthermore, failures are less frequent in the Great Belt VTS area compared to areas which are not actively monitored by the VTS.

Duration is another important aspect of failures. The failure type *miss of turning point* is fitted to a normal distribution, while the other failures are fitted to a lognormal distribution, although the lognormal distributions were obtained in different manners. In Paper I, this fitting of parameters was performed using the Python library SciPy's fitting algorithm (Virtanen et al., 2020), with the time expressed in hours; in Papers II and III, the log of time was used in the Python library NumPy (Harris et al., 2020), and the time was expressed in seconds. Table 4-3 summarises the distributions as presented in the different papers. Table 4-4 illustrates how many minutes until 50% of all failures were resolved.

Table 4-3. Statistical distributions and their parameters for durations of events (Halsafjorden, time in seconds; all others, time in hours). The parameters correspond to standard deviation σ, location τ, scale λ, and mean value μ (of the underlying distribution).

Event category	**Great Belt VTS**	**TSS Bornholmsgat**	**Halsafjorden**	**Rasmussen et al. (2012)**
Loss of propulsion	Lognormal, SciPy $\sigma = 0.71$ $\tau = 0.021$ $\lambda = 0.69$	Lognormal, SciPy $\sigma = 0.87$ $\tau = 0.1$ $\lambda = 0.97$	Lognormal, NumPy $\mu = 7.63$ $\sigma = 0.08$	Weibull $\sigma = 0.5$ $\lambda = 0.605$
Loss of steering	Lognormal, SciPy: $\sigma = 1.2$; $\tau = 0.06$ $\lambda = 0.54$			n/a
Miss of turning point	Normal $\mu = 0.064$ $\sigma = 0.015$	Normal $\mu = 0.19$ $\sigma = 0.047$	Normal $\mu = 360$ $\sigma = 54$	Less than 0.33 hours
WCT	n/a	n/a	Lognormal, NumPy $\mu = 4.8$ $\sigma = 0.7$	n/a
TWL	n/a	n/a	Lognormal, NumPy $\mu = 4.3$ $\sigma = 0.41$	n/a

Table 4-4. Minutes until 50% of all failures were resolved.

Event category	**Great Belt VTS**	**TSS Bornholmsgat**	**Halsafjorden**	**Rasmussen et al. (2012)**
Loss of propulsion	62	41	34	60
Loss of steering	45			n/a
Miss of turning point	3.8	11	6.0	20
WCT	n/a	n/a	2.5	n/a
TWL	n/a	n/a	1.5	n/a

Table 4-4 shows the large variation in failure duration across the different types of failures at the different locations. Specifically, the *loss of propulsion* and *loss of steering* failures last longer than the other types of failures. In the area actively monitored by the VTS in the Great Belt, the duration of the failure *miss of turning point* is shorter compared to the other locations.

The methods to detect these failures not only obtained their probabilities and durations but also enhanced the understanding of their behaviour. This understanding is key to establishing realistic settings when implementing such failures in the simulator autopilot.

4.2 Summary of Paper I – A method for risk analysis of ship collisions with stationary infrastructure using AIS data and a ship manoeuvring simulator

The main objective of Paper I is to create a new methodology for estimating the probability of allision. This methodology uses AIS data and a ship manoeuvring simulator to calculate the probabilities of grounding and allision in coastal waters. The method to quantify the duration and the frequency of passive failures (described in Section 3.2) is developed in this paper; furthermore, the paper describes the method developed to generate the starting input parameters and to run simulations in fast-time based on these inputs (outlined in Section 3.3). Regarding allision probability, this paper only includes passive failures; regarding consequences, it is limited to describing the size and speed of the striking vessels.

4.2.1 Case study – The Great Belt Bridge

The methodology developed in Paper I was examined using the Great Belt Bridge in Denmark (see Figure 4-1) as a case study. This area was selected because it was previously used in Pedersen's (1995) research regarding accident probability. The Great Belt Bridge area was studied through ten simulation sets divided into three categories, the results of which are presented in Table 4-5. The first category was used to investigate the randomness in the simulation caused by the Monte Carlo simulation of input parameters; for the simulations in this category, only the seed number was changed between the scenarios. The second category was used to analyse the sensitivities of failure frequency and failure duration; here, the same seed was used, but the frequency and/or the duration were altered in the generation. In the final category, two risk mitigation options were evaluated using the proposed methodology; these options were examples used in other locations to reduce risk.

1. **Investigation of random seeds**
   - A. Seed 1
   - B. Seed 2
   - C. Seed 3
2. **Sensitivity study of the parameters**
   - A. Increased drifting frequency and duration
   - B. Increased frequency for sharp turning ships
   - C. Increased frequency and duration for miss of turning point
   - D. Increased frequency for miss of turning point
   - E. Increased duration for miss of turning point
3. **Evaluation of risk mitigation options**
   - A. 12-knots speed restriction in the Great Belt VTS area
   - B. New layout of the routes, creating a longer straight sailing approach to the bridge

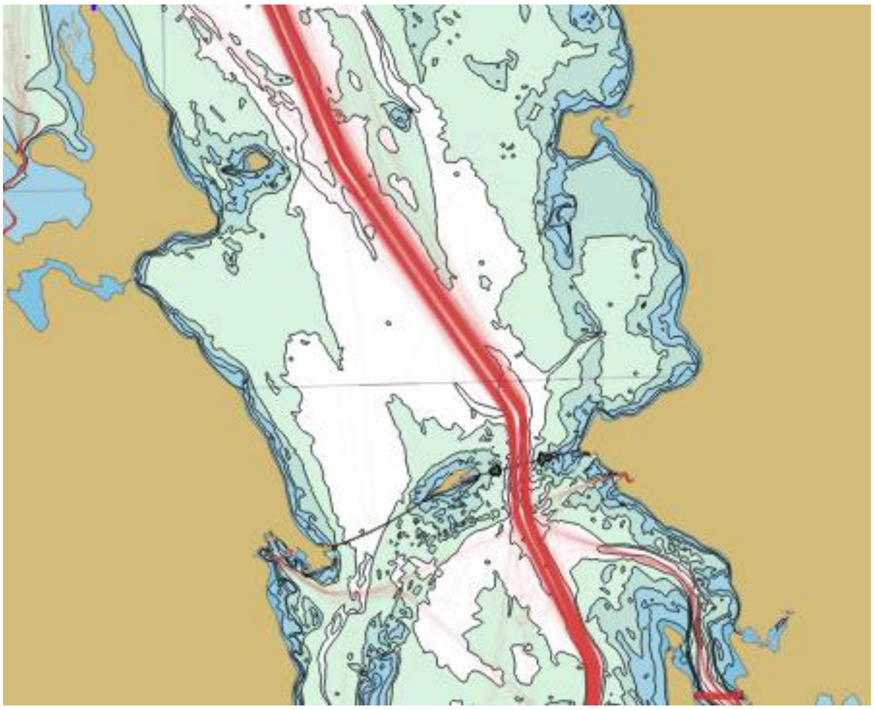

Figure 4-1. Ship traffic (red lines) passing the Great Belt Bridge in Denmark.

Table 4-5. Results from all simulation sets with Y_{rep} = 100,000; number of allision accidents caused by LP = loss of propulsion, LS = loss of steering, MTP = miss of turning point.

Id	Number of simulations	Number of groundings	Number of allisions (LP, LS, MTP)	Maximum allision energy (MJ)	1,000-year expected allision energy (MJ)
1.A.	3,959,282	50,258	710 (376, 85, 249)	3,221	1,667
1.B.	3,959,282	51,198	722 (385, 97, 240)	4,634	1,601
1.C.	3,959,282	51,206	730 (395, 87, 248)	2,708	1,605
2.A.	4,221,089	65,516	985 (651, 85, 249)	3,221	1,667
2.B.	3,994,525	54,268	800 (376, 175, 249)	3,221	1,667
2.C.	5,169,542	1,020,580	27,954 (376, 85, 27,493)	4,822	4,268
2.D.	5,169,542	60,662	777 (376, 85, 316)	3,221	1,880
2.E.	3,959,282	748,053	20,606 (376, 85, 20,145)	5,054	4,179
3.A.	3,959,282	32,003	436 (347, 89, 0)	1,030	12
3.B.	3,962,135	50,255	484 (402, 82, 0)	2,258	22

The number of simulations to run in each set was calculated according to Eq. (3.1), using 100,000 times as Y_{rep}. An initial test with Y_{rep} set to 10,000 times was first evaluated using sets 1.A–1.C; however, this resulted in a larger spread between the different seeds than the criterion given in Eq. (3.4). Consequently, Y_{rep} was raised to 100,000 times, and the variation between the random seed became less than 5%, thereby meeting the criterion for Eq. (3.4).

The results of Scenarios 1.A., 1.B., and 1.C. also showed that the probability of grounding is 0.51 per year (the average number of groundings in these scenarios was 50,887, and the simulations represent one year 100,000 times). This corresponds well with the accident statistics from the area, wherein five groundings were reported during a ten-year period (IHS Fairplay, 2020) (assuming that the amount of traffic was relatively constant in this period).

In Scenarios 2.A–2.E, failure statistics from the TSS Bornholmsgat were used to investigate the sensitivity of the methodology to the failure statistics. In Scenario 2.A, both the frequency and the duration of *loss of propulsion* were increased; this led to a 30% increase in the number of groundings but did not affect the allision energy. Scenario 2.B produced a similar result, where the *loss of steering* frequency was increased by 50% but the increase in the number of groundings was by only a few percentage points. The result of Scenario 2.C, with increased frequency and duration of the event *miss of turning point*, differs more from Scenario 1 than Scenario 2.A and 2.B; for this reason, Scenario 2.C was divided into 2.D—increased frequency—and 2.E—increased duration. The result of Scenario 2.D showed an increase in the number of groundings by 20% and one in the allision energy by 12%. The average duration for the failure *miss of turning point* was 3.83 minutes. Increasing this duration to 11.4 minutes in Scenario 2.E had a major effect on the results: the number of groundings increased 1,048%, and the allision energy increased by 250%.

The two mitigation scenarios—3.A–reduction in the maximum allowed ship speed, and 3.B–change of the navigation path—illustrate how this methodology can be utilised. Both mitigation strategies were successful in reducing the expected allision energy. They are included as realistic examples of risk mitigation options; however, further analyses are recommended to capture their impact on ship traffic.

4.2.2 Concluding remarks

The Great Belt VTS area was used as a case study in Paper I. Three failure types were identified and quantified in terms of frequency and duration. It should be noted that the frequency of these events differs between the Great Belt VTS and the TSS Bornholmsgat. To check the validity of the simulation, the number of groundings were compared with real-world statistics. When 100,000 simulations of one-year ship traffic were run, the resulting number of groundings corresponded well with the accident statistics from the past ten years. It was concluded that the methodology presented in this paper can be used to simulate and analyse traffic scenarios in coastal waterways to calculate the probability that a ship accident will occur. The sensitivity study in this paper highlighted that the duration of the event *miss of turning point* is the most sensitive parameter to the methodology. The suggested mitigation actions were not analysed to judge whether the consequences of these measures are less severe than the consequences of potential ship-bridge allision; however, these risk control options are worth investigating further, based on the allision probability with the present ship traffic.

One important aspect of risk estimation is the uncertainty associated with the frequency of ship-bridge allision events. The results from the sensitivity analysis in Scenarios 2.A–E clearly demonstrate how variations in failure frequency and duration assumptions affect the estimated accident probability. This highlights the importance of carefully defining input parameters and understanding their influence on the model's outcome. While the STAPS methodology incorporates realistic failure statistics derived from AIS data, uncertainties remain due to the rare nature of these events. Future work could define a minimum number of failures required to build reliable statistics, as well as propose strategies for obtaining such data—either by expanding the geographical scope or by extending the temporal range of AIS records. These efforts would further enhance the robustness and transparency of the methodology.

A problem with the existing framework for allision risk assessment is that the probability and the consequence of events often are treated separately. The methodology proposed in Paper I reduces this problem. Even though the methodology focuses on probability, it includes the kinetic energy of the ship prior to the allision, and all parameters from the ship needed for structural analysis are available for further analysis.

Finally, in the paper, it was concluded that the methodology can be applied both in the planning phase of a new bridge over a waterway and in the assessment of existing ship routes near bridges where ship traffic has changed since the bridge's construction. This methodology is not limited to ship-bridge allisions: it can also be used to assess the probability of allisions with other offshore infrastructure or of other maritime accidents, such as ship groundings.

4.3 Summary of Paper II – Probability of active navigational failure

On 2 March 2023, the Bergsøysundbrua in Norway was struck by a small cargo vessel. Although the ship was relatively lightweight and the resulting damage was minor, its trajectory could not be explained by previously-investigated passive failures. This incident highlighted the need to investigate additional types of failures. Thus, the primary objective of Paper II is to analyse the frequency of active navigational failures. In the risk model presented by Pedersen (1995), these failures were referred to as *ships off-course* and were assumed to account for 2% of all ships (Karlsson et al., 1998; Pedersen et al., 2020). The method developed in Paper II, to obtain these active failures relies not only on AIS data but also on accident and incident reports, as described in Section 3.2.

4.3.1 Case study – Scandinavia

Accident databases were investigated to identify Scandinavian allision accidents between 2006 and 2023. Four databases were used for this investigation: IHS Fairplay (2023), EMCIP (2023), Sjøfartsdirektoratet (2023), and GISIS (2023). In the GSIS database, no ship-bridge allision accidents were found among the contact accidents in Scandinavia after 2006, and 11 allision accidents were identified in the remaining investigated databases and from AIS tracks from Scandinavia in 2006–2023 (see Figure 4-2). The AIS tracks of these 11 accidents were analysed, and the accidents were categorised (see Table 4-6) based on the failures illustrated in Figure 3-4. In short, the failures behind these allisions were: 1 *loss of propulsion* failure, 3 *miss of turning point* failures, 5 active navigational errors, and 2 unknowns. The two allisions classified as "unknown" involved a search-and-rescue ship and a tugboat, respectively, and it was not possible to put them into one of the failure categories based on their AIS data.

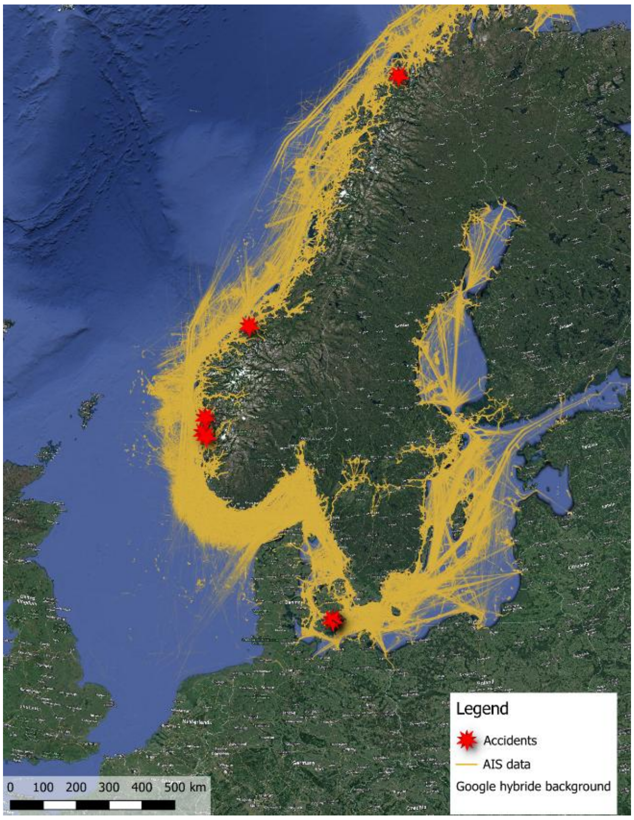

Figure 4-2. Accident locations in Scandinavia with AIS data.

Table 4-6. Allisions in Scandinavia where AIS tracks have been identified, based on accident records from IHS Fairplay (IHS), EMCIP, and SjøfartsDirektoratet (SD). *Yearly passages refer to the average in 2018–2022; for Masnedsundbruen and Bergsøysundbrua (bridges not intended to have ships passing underneath), the traffic passing outside is quantified instead.

Database	Date	Bridge	Ship length [m]	Accident type	Yearly passages*	Opened
SD	2009-06-02	Nordhordalsbrua, NO	67	Miss of turning point	9,738	1992
IHS	2011-10-27	Storstrømsbron, DK	88	Navigational error, WCT	1,722	1937
SD, IHS	2013-02-03	Storholmbrua, NO	57	Miss of turning point	2,593	2007
SD	2014-12-23	Tromsö, NO	46	Navigational error, WCT	11,488	1960
EMCIP	2015-09-18	Masnedsundbroen, DK	90	Loss of propulsion	4,925	1937
IHS	2015-10-03	Färö bridge, DK	88	Navigational error, WCT	1,705	1984
SD	2017-06-16	Bårdsundsveg, NO	27	Unknown	199	1950
SD, IHS	2019-06-06	Nordhordalsbrua, NO	80	Miss of turning point	9,738	1992
EMCIP	2019-10-13	Andøybrua, NO	68	Navigational error, WCT	3,288	1974
SD	2021-06-27	Åkviksundet, NO	16	Unknown	78	1999
IHS	2023-03-02	Bergsøysundbrua, NO	50	Navigational error, TWL	1,099	1992

Defining accident frequency based on the data in this study is problematic, because bridges may have experienced more accidents than are found in the accident databases and because ship traffic volume has increased since the bridges were built. Eidem et al. (2023) exemplified the latter through the example of Nordhordlandsbrua, where the ship traffic has increased and thus the probability of an allision greater than 25 MJ is 10 times higher today than it was in 1992, when the bridge was completed.

The incident reports from the ship traffic in the Great Belt were included to complement the accident analysis in Paper II. Between 1 September 2021 and 31 March 2023, the Great Belt VTS issued 87 incident reports; of these, 56 were available for this study (the remaining 31 incident reports were unavailable for legal reasons). These 56 incidents reports were combined with AIS data to categorise the failures. Table 4-7 summarises the categorisation of the causes of these 56 incidents. The incident probability in the table was estimated by dividing the number of events by the total number of hours ships spent in the area, which is estimated based on AIS data. In total, commercial traffic spent approximately 150,000 hours in the VTS area in 1 September 2021–31 March 2023. The frequency of the events is expressed per hour in Table 4-7, although *miss of turning point* and *WCT* are expressed per turn; the number of turns per hour a ship is required to perform while transiting the VTS area depends on which route the ship intends to follow, the ship speed, etc., but it can be roughly approximated as 2 turns per hour. During the period covered by the VTS incident reports, no accidents were found in the Great Belt VTS area in the studied databases.

Table 4-7. Summary of VTS reports. The failure frequency is the number of reports/total number of hours.

Description	# Reports	Frequency/hour	Frequency/turn
Meeting incidents, avoiding ship-ship collisions	19	-	-
Pleasure crafts, communication errors, destruction of AtoN, etc.	11	-	-
Blackout	5	3.3×10^{-5}	-
Steering problem	2	1.3×10^{-5}	-
Miss of turning point	4	2.7×10^{-5}	1.3×10^{-5}
Navigational error, WCT	8	5.3×10^{-5}	2.7×10^{-5}
Navigational error, TWL	7	4.7×10^{-5}	-

Ten bridges in Scandinavia which have experienced allisions due to active navigational errors or similar bridge layouts were also studied in this paper, using AIS data. The AIS data used in this case study spans from 1 January 2017 to 31 March 2023, and the results are presented in Table 4-8.

The *TWL* error was searched for at four bridges (and at one bridge, in both directions). Of the nearly 40,000 passages at these bridges, four AIS tracks were identified as *TWL* errors, resulting in a frequency of 1×10^{-4} per passage. However, this failure type is assumed to occur at any given point along the path and is therefore expressed per hour: assuming that a passage takes 10 minutes, this results in a frequency of 1.5×10^{-4} per hour.

The *WCT* error was searched for at six bridges (and at one bridge, in both directions). In total, approximately 130,000 turns were included in this study; of these, 13 AIS tracks were identified as *WCT* navigational errors, resulting in a frequency of 1×10^{-4} per turn. The course failure in these cases was 1–6 degrees offset compared to the “normal course”. The difference between heading and COG was also studied for these 13 failures; in 8 of these cases, the difference corresponded to the drifting angle, which indicates that the ship failed to account for the drift.

Table 4-8. Identification of active navigational errors close to bridges in Scandinavia. *The total number of passages refers to the number of ships travelling between 2017-01-01 and 2023-04-01. **The number of allisions which happened before 2017 are in parentheses. ***The allision at the Norhorlandsbrua was classified as a *miss of turning point* failure.

Name of bridge	**Country**	**Traffic from**	**Error type**	**Total number of passages***	**Number of candidates**	**Number of allisions ** **	**VTS**
Bergsøysundbrua+ Gjemnessundbrua	Norway	North	TWL	3,813	2	1	No
Bergsøysundbrua+ Gjemnessundbrua	Norway	South	TWL	1,166	2	0	No
Nordhordalsbrua	Norway	East	TWL	31,615	0	1 (1) ***	No
Sandhornøybrua	Norway	North	TWL	30	0	0	No
Sundklakkbrua	Norway	South	TWL	3,234	0	0	No
Tromsøbrua	Norway	North	WCT	23,889	2	0	No
Tromsøbrua	Norway	South	WCT	21,792	2	0	No
Great Belt Bridge	Denmark	North	WCT	46,865	2	0 (2)	Yes
Farøbroerne	Denmark	West	WCT	4,811	1	0 (1)	No
Storstrømsbroen	Denmark	West	WCT	4,560	5	0 (1)	No
Öresundsbron	Sweden	North	WCT	21,248	0	0	Yes
Ölandsbron	Sweden	South	WCT	6,734	1	0	No

The duration of the failures—i.e., the time from when the turn occurred to when it was corrected—was also measured for the incidents and failures. The scatter plot in Figure 4-3 illustrates the times, arranged from the fastest to the slowest detection of failure. The figure also contains a lognormal distribution representing each scatter plot. Here, μ is the mean and σ is the standard deviation of the normal distribution of the logarithm of the variable.

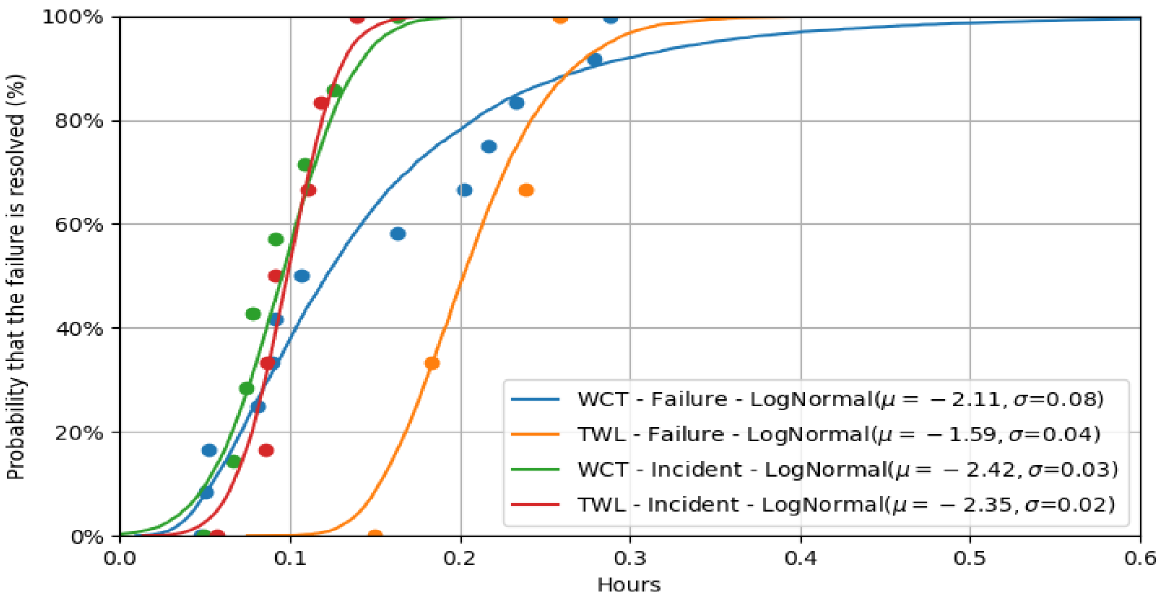

Figure 4-3. Scatter plot with *WCT* and *TWL* failures, including a lognormal distribution.

The number of failures is too few to make any strong claims regarding failure duration. However, the resolution time of the incidents (green and red lines) compared with the resolution time of the failures (blue and orange) indicates that the area under surveillance by the VTS tends to see courses corrected faster than other locations. Specifically, most of the observed incidents and failures were resolved in 5–15 minutes. The *WCT* failure has the longest duration, probably because a small deviation from normal behaviour is more difficult to detect than a large deviation.

4.3.2 Concluding remarks

Risk assessments of ship-bridge allisions address several types of risks. The aim of this paper was to investigate the current practices for modelling active navigational errors with respect to their behaviour, frequency, and duration. Active navigational errors were divided into *WCT* (Wrong Course at a Turning point) and *TWL* (making a Turn at the Wrong Location).

This research revealed that the standard assumption of a uniform distribution of active navigational failures as 2% of total traffic volume does not provide an accurate estimation. Instead, in the studied areas surrounding selected bridges in Norway, Sweden, and Denmark, the frequency of active navigational errors is closer to 0.01% per passage. However, given that a ship experiences one of these failures, Paper II indicates that the causation factor is approximately 0.2, compared to the standard assumption of 1.6×10^{-4}. This combination of a reduction in the event frequency and an increase in the causation factor keeps the accident frequency within the same range as current practice, but it provides a more realistic representation of the situation.

The research also revealed that the probability of this type of incident varies greatly from bridge to bridge, depending on the geometrical layout of routes and the locations of bridges in relation to the routes. VTS and Aids to Navigation (AtoN) are important factors for decreasing accident and failure rates. Areas with islands, which could mislead the navigator, increase the probability of incidents. The current practice, which uses a uniform distribution of 2% of the traffic, seems to be unreasonably conservative for most bridges, which could result in fewer bridges undergoing adequate risk analysis. It is recommended that risk assessments for allisions tailor both the failure frequency and the causation factor in relation to the local characteristics, since each area is unique. Further research is recommended to define different types of failure even more clearly, in order to avoid any potential overlaps between different failure categories.

4.4 Summary of Paper III – Probabilistic analysis of ship-bridge allisions when designing bridges

Paper III has two objectives: first, to incorporate the active navigational errors from Paper II into the methodology presented in Paper I, thereby creating the STAPS methodology; second, to compare this methodology with the existing IWRAP Mk II software. This comparison between STAPS and IWRAP Mk II is performed using two different case studies.

4.4.1 Case study 1 – Simulation of one bridge with one leg

To investigate the hydrodynamic simplifications in IWRAP Mk II, a case study was created in which drifting behaviour was analysed in three scenarios and powered accidents in one scenario. Each of the four scenarios consisted of a single 1,000-meter leg (the route where the ship travels) and an equally long bridge (with the bridge being lower than the ship—i.e., the ship cannot pass under it). This case study setup is not realistic, since both the leg and the bridge start and stop in the middle of the ocean; however, the accident probability could be estimated regardless. Each of the four scenarios was run nine times, with three different distances between the bridge and the leg (1, 3, and 5 nm apart) and with three different models (IWRAP MkII, Seaman using a 90-m-long ship, and Seaman using a 225-m-long ship).

The four scenarios were described in the paper as:

- **Scenario 1.1:** Limited drift direction and limited start speed
  The drift (in IWRAP Mk II) and current (in STAPS) directions were equally divided into eight distinct directions in both models (see Figure 5). In IWRAP Mk II, the drift speed was set to 1 knot, and in STAPS, the current speed was set to 1 knot, in order to make the conditions as similar as possible between the models. This scenario should be regarded as the base case in relation to Scenarios 1.2 and 1.3.
- **Scenario 1.2:** Unlimited current directions in STAPS but limited start speed
  The same settings as in Scenario 1.1 were used, but in this scenario, STAPS was not restricted to distinct current directions (a change that is not possible in the IWRAP Mk II software). This scenario aimed to quantify the effect of the limitation of distinct drifting directions with this case setup.
- **Scenario 1.3:** Unlimited current direction and normal start speed in STAPS
  The same settings as in Scenario 1.1 were used, but in this scenario, STAPS was not restricted to distinct current directions or the 1-knot starting speed (a change that is not possible in the IWRAP Mk II software). The ships were instead initiated at 15 knots without propulsion in the leg direction and 1 knot current speed, the current direction which was evenly distributed.
- **Scenario 1.4:** Powered accident
  In this scenario, the leg was rotated 90° and directly pointed at the bridge, ensuring that the ships which failed would strike the bridge at full speed. This scenario revealed that powered accidents due to missed turns were estimated in similar manners in both models.

The layout of this case study, with the leg in the centre and the eight drift directions, is illustrated in Figure 4-4.

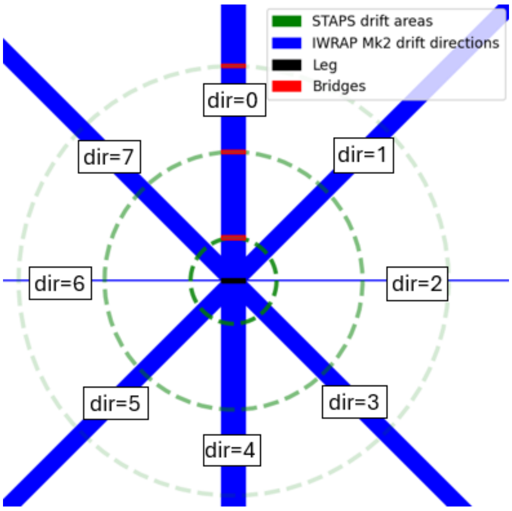

Figure 4-4. The three bridges (red) and the leg (black) in Scenarios 1.1–1.3. The blue areas indicate where ships may drift from a 1,000-meter-long leg in IWRAP Mk II (dir[0-7]×45°). The ships may drift in any direction in STAPS (except in Scenario 1.1). The growing opacity of the green circles indicates the decreasing proportion of the bridge length has on the total circumference. Figure reused from Paper III.

Before the scenarios were run in STAPS, Y_{rep} was defined using Eq. (3.4); for Scenarios 1.1–1.3, Y_{rep} was defined as 10^7 yielding 61,640 *loss of propulsion* simulations, and for Scenario 1.4, Y_{rep} was defined as 10^6 yielding 160,000 *miss of turning point* simulations, per distance and ship type.

The allision probabilities for all the simulated scenarios are presented in Table 4-9. The models were differently affected by the distance between the leg and the bridge. Figure 4-5 presents examples of the results from Table 4-9 in a bar plot—specifically, for the case when the leg and the bridge were separated by 3 nm. This distance was chosen as a representative example to illustrate the results, as it provides a balanced view between the shorter (1 nm) and longer (5 nm) distances.

Table 4-9. Probability of allision for the different scenarios in Case Study 1.
The numbers present the allision probabilities per year.

Model	**IWRAP Mk II**			**STAPS, 90 m ship**			**STAPS, 225 m ship**		
Distance	1 nm	3 nm	5 nm	1 nm	3 nm	5 nm	1 nm	3 nm	5 nm
Scenario 1.1	2.6×10^{-4}	4.3×10^{-5}	8.1×10^{-6}	2.7×10^{-4}	4.7×10^{-5}	9.0×10^{-6}	2.7×10^{-4}	4.7×10^{-5}	9.0×10^{-6}
Scenario 1.2				1.9E$\times10^{-4}$	1.1×10^{-5}	1.1×10^{-6}	2.1×10^{-4}	1.3×10^{-5}	1.3×10^{-6}
Scenario 1.3				8.5×10^{-5}	5.4×10^{-6}	0.3×10^{-6}	2.2×10^{-6}	1.6×10^{-6}	0.6×10^{-6}
Scenario 1.4	5.9×10^{-2}	4.1×10^{-3}	2.8×10^{-4}	6.4×10^{-2}	4.1×10^{-5}	3.0×10^{-4}	6.6×10^{-2}	4.2×10^{-3}	3.2×10^{-4}

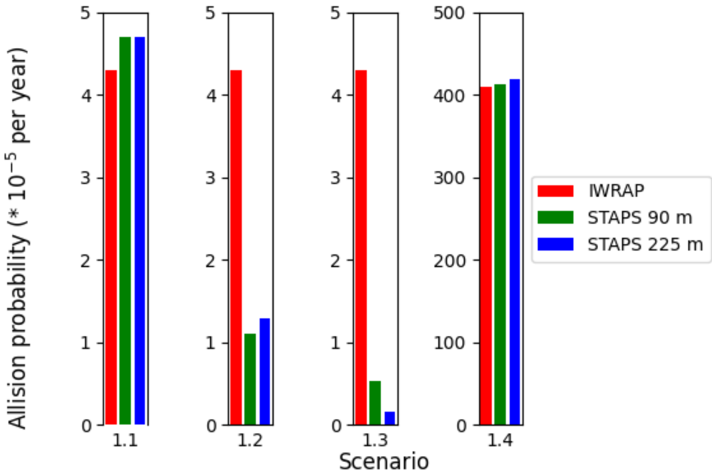

Figure 4-5. The probability of allision in Scenarios 1.1–1.4 when the leg and bridge are 3 nm apart. Figure reused from Paper III.

The results of Scenario 1.1 showed that the drift probabilities in IWRAP Mk II and STAPS were similar; the small difference in the results was caused by the randomness in the number of "long" simulations with the northbound current which were simulated in STAPS. However, in Scenarios 1.2 and 1.3, when the drifting direction was not restricted in STAPS, there was a large difference between the IWRAP Mk II and STAPS results. As the distance increased, the differences between the scenarios and models also increased, which is to be expected since the bridge becomes a smaller part of the circle circumference (see Figure 4-4).

Comparing the two ship sizes in STAPS, Scenario 1.2 showed that the 225-m ship has a slightly higher probability of allisions than the 90-m ship. This difference is due to ship geometry: the 225-m ship strikes the bridge in a slightly larger sector than the 90-m ship. A larger difference in allision probability was observed when the initial ship speed was set to the operational speed in Scenario 1.3; this is because the larger ship has a larger mass travel for a longer time in the leg direction before it starts to drift.

The results from Scenario 1.4, the powered allision, were almost identical in IWRAP Mk II and STAPS. The minor difference—a slightly higher probability of allisions in STAPS than in IWRAP Mk II—is explained by how the ship geometry is modelled in the different models. In IWRAP Mk II, the distance between the end of the leg and the bridge is used, whereas in STAPS, the geometry of the ship is modelled, which means that the bow is approximately half of the ship's length closer to the bridge. This also explains why the larger ship had a higher accident probability.

4.4.2 Case study 2 – Simulation of a real-world scenario

A potential bridge over Halsafjorden (Norway) was selected as the realistic example for the second case study. It is located on the west coast of Norway, between Bergen and Trondheim (see Figure 4-6 left). In order to represent a realistic analysis, the case study comprises multiple legs, different types of vessels, the annual dominant current and wind directions in the area, as well as additional types of failures. Figure 4-6 (right) shows the fjord's layout, including the potential bridge (blue line), AIS tracks (thin red lines) of today's ship traffic, and three legs (thick red lines) indicating how future ship traffic may travel if the bridge is built. (The red solid elliptical shape south of the bridge is the ferry operating in the area today.)

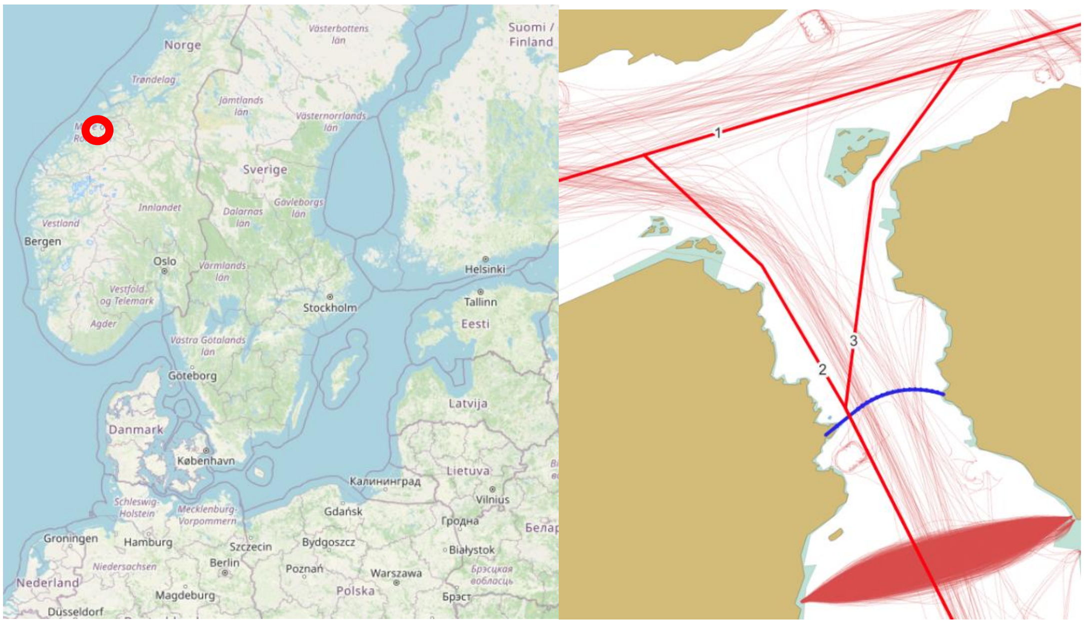

Figure 4-6. (Left) Overview map; the red circle indicates where the Halsafjorden is located in Norway. (Right) The ship traffic (red) in the Halsafjorden during June 2023, including legs and the new bridge (blue) layout. Figure reused from Paper III.

Four scenarios were designed, wherein Scenario 2.1 was the baseline case with the primary purpose of benchmarking the IWRAP Mk II and STAPS models for more realistic scenarios compared to Case Study 1. Scenarios 2.2, 2.3, and 2.4 can be understood as parametric, sensitivity, and mitigation action studies, respectively.

- **Scenario 2.1: Baseline case**
  In this scenario, the model used the settings presented in Section 4.1.
- **Scenario 2.2: Without active navigational errors**
  In this scenario, the same model settings as in Scenario 2.1 were used, except that the frequency of *WCT* and *TWL* failures were set to zero in STAPS and the "fake leg" spanning the entire bridge was removed in IWRAP Mk II.
- **Scenario 2.3: Increased *miss of turning point* failure duration**
  In this scenario, the same model settings as in Scenario 2.1 were used, except that the duration of the *mean time between checks* parameter in IWRAP Mk II was increased to 240 seconds (from 180 seconds) and the normal distribution in STAPS was increased to μ = 420 seconds and σ = 114 (from μ = 360 seconds and σ = 54).
- **Scenario 2.4: Introduction of VTS and TSS**
  This scenario was based on a change in the layout of the fairway and reduced probabilities/durations of active navigational failures.

The results, presented in Table 4-10, revealed some major differences in the probability of allision accidents between the different scenarios and between the two models. IWRAP Mk II always predicted a higher accident probability than STAPS, although both models showed similar trends between the different scenarios—i.e., an increase or a decrease of allision probability compared to the baseline case. They also provided the same ranking in allision probabilities: in descending magnitudes, Scenarios 3, 1, 2, and 4.

Table 4-10. Summary of allision probabilities computed by IWRAP Mk II and STAPS.

	Allision probability (per year)			
Scenario	**2.1**	**2.2**	**2.3**	**2.4**
IWRAP Mk II	6.3×10^{-3}	4.8×10^{-3}	1.0×10^{-2}	1.7×10^{-3}
STAPS	1.4×10^{-3}	6.2×10^{-4}	5.9×10^{-3}	5.8×10^{-4}

The results presented in Table 4-10 revealed that active navigational errors (comparing Scenario 2.2 and 2.1) had an impact on both the IWRAP Mk II and the STAPS results, errors causing powered accidents. Scenario 2.3 compared with Scenario 2.1 indicates that the duration of the *miss of turning point* failure is an important parameter (a similar conclusion was in Paper I); this is further illustrated in Figure 4-7, which shows how the probability of a *ship continuing to travel pass the turning point* decreased with distance with the different failure durations. (A ship travelling at 11 knots was used in the demonstration.) The blue and orange lines represent the baseline case and the increased duration time in IWRAP Mk II, respectively, and the green and red lines represent the baseline case and the increased duration time in STAPS, respectively.

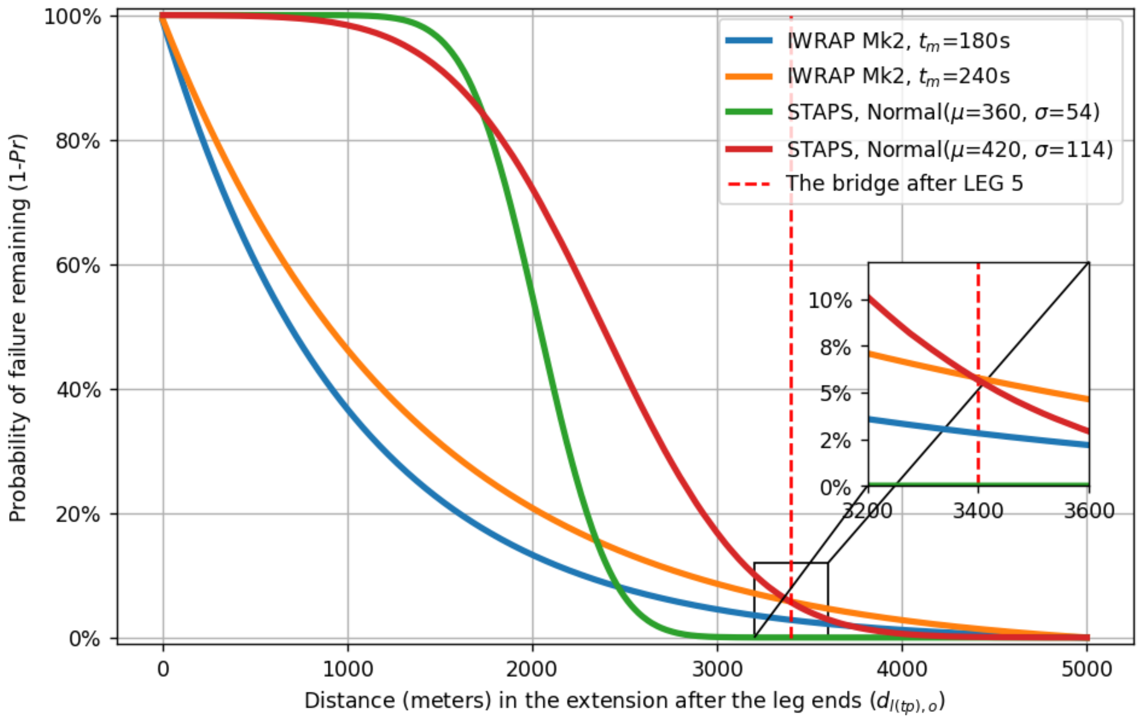

Figure 4-7. The probability of failure remaining for a ship travelling at 11 knots depending on the distance, with different failure functions. The red dotted line marks the distance between the crucial turning point and the bridge. Figure reused from Paper III.

As illustrated in Figure 4-7, the 60-second increase in duration for the *miss of turning point* failure increased the probability that the failure continued at the distance where the bridge is located (red dashed line). Since the ship speed is a random parameter in STAPS, this figure is just one example involving a ship at 11 knots; ships with higher speeds will strike the bridge due to a *miss of turning point* failure even with the base case duration.

The modelling of future ship routes involves uncertainty, as the exact coordinates of a planned layout are sensitive to the analyst's assumptions and experience. In order to quantify this sensitivity, ten experts on maritime risk assessment were invited to a route layout benchmark study, applying the baseline scenario in Case Study 2. Five of the experts were employed at the Research Institutes of Sweden (RISE), and five were international experts from different European countries. The experts worked independently, and they were given the same basic information regarding the AIS ship traffic data, the topology in the area, and the bridge layout. Figure 4-8 presents a summary of the participants' suggestions for the coordinates of Routes 2 and 3. Since there is no "correct way" to model how future traffic will navigate around a planned bridge, the experts used their experience to define the future routes.

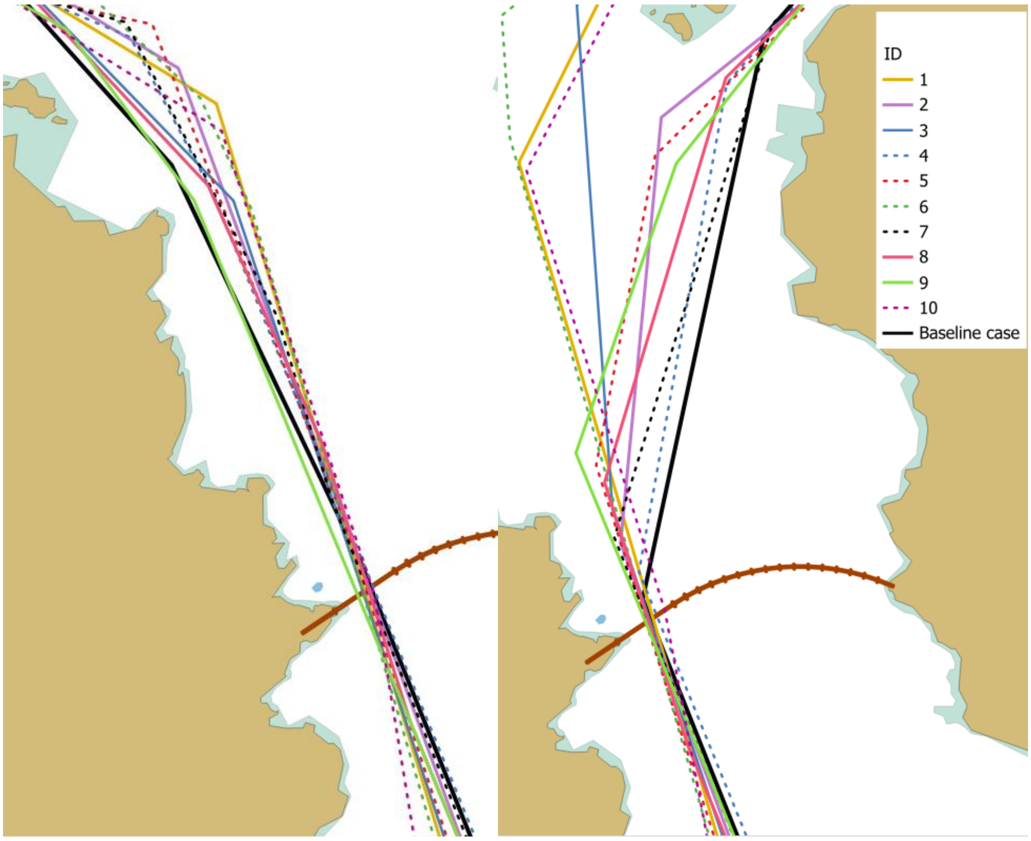

Figure 4-8. The baseline case, (left) Route 2 and (right) Route 3, and the 10 experts' alterations of these routes. Figure reused from Paper III.

Both IWRAP Mk II and STAPS were used to quantify how the experts' route geometries affected allision probability. All simulations were run with the same settings as Scenario 2.1. The results from the 10 experts' routes, together with those from Scenario 2.1, are presented in Table 4-11.

Table 4-11. Number of expected allisions with the layouts given by the 10 experts, using $Y_{rep} = 10^6$ in STAPS and during 10^6 years in IWRAP Mk II.

Model	Scenario 2.1	1	2	3	4	5	6	7	8	9	10
IWRAP Mk II	6,310	2,800	3,300	6,200	3,700	3,400	3,300	5,200	3,700	2,600	9,400
STAPS	1,435	665	1,112	4,254	2,955	619	2,889	17,216	2,110	1,539	3,745

As illustrated by the sensitivity results presented in Table 4-11, the design of the future routes had a large impact on the expected number of allisions. In IWRAP Mk II, the average number of expected allisions on the experts' route designs was 4,354; the most successful route design only had 2,600 expected allisions, and the worst design had 9,400. In STAPS, the numbers ranged from 619 to 17,216, with an average of 3,710 expected allisions.

The large differences in the results for the different route designs demonstrate that future route coordinates have a major impact on the accident probability. Therefore, it is important to understand how these coordinates are interpreted and influence the output of each model. The simplification of hydrodynamic effects in IWRAP Mk II was highlighted in the former section as a major cause of the difference between the two models. Nevertheless, in this particular base layout, an additional factor likely outweighs the influence of hydrodynamic effects in explaining the difference between the models—a factor related to the failure duration and the distance between the waypoints and the bridge. The route suggestions from Participants 1 and 5 had low numbers of accidents as a result of layouts lacking routes pointing towards the bridge, whereas the layout from Participant 7 contained waypoints closer to the bridge, where most of the *miss of turning point* and *WCT* failures remained unsolved. The dotted line in Figure 4-7 illustrates a specific distance and one instance of the remaining failure probability. However, each participant's route has a different geometry, resulting in varying probabilities of this failure persistence. Thus, for this specific layout, it is the failure duration that contributes mostly to the difference between the model.

4.4.3 Concluding remarks

In Paper III, two quantitative probability assessment models—IWRAP Mk II and STAPS—were applied to analyse the probability of ship-bridge allision in two separate case studies. These analyses enabled a comparative evaluation of the pros and cons of each model. The first case study focused on detailed differences, particularly how the inclusion of hydrodynamic effects and ship geometry influenced the risk assessments. The second case study, adopting a more holistic perspective, examined how the models performed in a real-world risk analysis context.

In the two case studies, IWRAP Mk II consistently estimated a higher probability of allisions than STAPS. In the first case study, this was primarily due to the absence of hydrodynamic calculations in IWRAP Mk II; in the second case study, it was linked to the lower fidelity in failure modelling in IWRAP Mk II. The findings demonstrate that increasing the fidelity in failure modelling reduces the model uncertainty and lowers the predicted accident probability.

A sensitivity analysis of the route layout in Case Study 2 revealed that route modelling significantly affects accident probability. This underscores the importance of accurately predicting future ship routes. The variation in the experts' forecasts further highlights the uncertainty involved in modelling future traffic patterns, particularly when routing systems are expected to change as a result of physical infrastructure modifications.

The comparative analysis reveals that STAPS is a more sensitive methodology than IWRAP Mk II, primarily due to its ability to model failure durations and ship behaviour with higher fidelity. This increased sensitivity stems from STAPS's capacity to incorporate hydrodynamic effects and probabilistic failure modelling, which enables more realistic risk estimates. While IWRAP Mk II offers faster computation and may be suitable for early-stage assessments, its reliance on historical accident data and simplified modelling limits its applicability in detailed design contexts. In contrast, STAPS simulates real-world failure scenarios and accounts for ship geometry, making it more reliable for defining accidental load cases and evaluating risk mitigation strategies. These strengths are particularly important across all layout types, as route geometry consistently influences accident probability. Therefore, STAPS is better suited for detailed design and risk mitigation studies related to bridge design, fairway layout, and ship operations.

4.5 Summary of Paper IV – Combined probability and consequence modelling of ship-bridge allisions

The main objectives of Paper IV are to add consequence assessments to STAPS—thereby forming the STAPS-cons methodology—and to analyse the risk of ship-bridge allisions. In this paper, Seaman's 2D time-domain simulation is used to run all scenarios until they end in either no accident, ship grounding, or ship allisions. The details of those ships involved in allisions are combined with the results from FEA simulations to form the STAPS-cons methodology, as described in Section 3.4.

4.5.1 Case study – The Bjørnafjorden crossing

To demonstrate the capabilities of the proposed methodology, this paper included a ship-bridge allision risk analysis for a real-world case study. Through this case study, Paper IV also assessed the sensitivity of three input parameters. The case study contains a potential bridge over the Bjørnafjorden, a fjord in the western part of Norway located between the cities of Stavanger and Bergen. In 2023, approximately 5,600 ships passed west of the bridge crossing, and almost 2,000 ships passed through Bjørnafjorden. Figure 4-9 illustrates the AIS tracks from July 2023, with four *passage lines* (I–IV) and future routes (1–5). The failure frequencies applied in the analysis of these routes were gathered from Papers I, II, and III. This planned bridge has also been studied by others who found the maximum capacity of the bridge, including Yu et al. (2024) and Storheim et al. (2019); based on these studies, C_l was set to 50 MJ and C_g was set to 160 MJ for the maximum capacity used in Eq. (3.8).

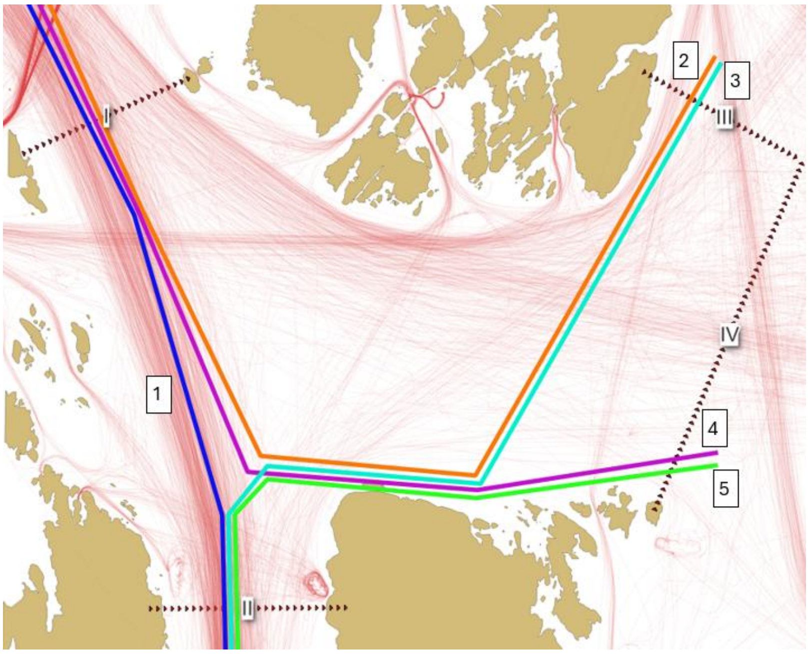

Figure 4-9. Map over the Bjørnafjorden area with AIS data during July 2023 (excluding road ferries), the four passage lines (I–IV), and five future routes (1–5); these lines are slightly offset from their original position in order to be visualised. Figure reused from Paper IV.

For the analysis of the sensitivity of the risk assessment, two parameters related to the probability estimation and one related to the consequence estimation were altered. In total, five scenarios were investigated:

1. Baseline
2. Increased frequency of *miss of turning point* failure
3. Increased duration of *miss of turning point* failure
4. A less stiff structure, reduced energy uptake in the global model
5. A stiffer structure, increased energy uptake in the global model

For this analysis, Y_{rep} in Equations (3.2) and (3.3) was set to 10^6 years, which yielded in approximately 15,000,000 STAPS simulations for Scenarios 1, 2, and 3, while Scenarios 4 and 5 used the allisions from Scenario 1. This resulted in 1007 allisions for Scenarios 1, 4, and 5, 1,035 allisions for Scenario 2, and 1,398 allisions for Scenario 3.

The remaining kinetic energy of the ships involved in allisions, $K_{pos,ship}$, was obtained using Eq. (3.7). This $K_{pos,ship}$ was combined with the FEA simulations by Jin et al. (2020) to distinguish between the different energy components in Eq. (3.6) depending on different angles of attack for the pontoon allisions and different impact locations along the bridge beam. With all energies known, the number of allisions above the bridge's maximum capacity (either local or global) could be found using Eq. (3.8). In Scenario 1 (the baseline case), 81 allisions were found wherein the maximum energy was above 50 MJ for C_l or 160 MJ for C_g, which means a probability of bridge collapse of 0.81×10^{-4} per year. However, C_l and C_g could be adjusted in the final design (e.g., increased/decreased shell thickness); how such design alterations affected $N_{collapse}$ in the baseline is illustrated in a 3D surface in Figure 4-10 (Paper IV includes similar figures for each scenario). The black line illustrates where the surface crosses the level of 100 collapses in 1,000,000 years, which corresponds to the Norwegian 10^{-4} design criteria.

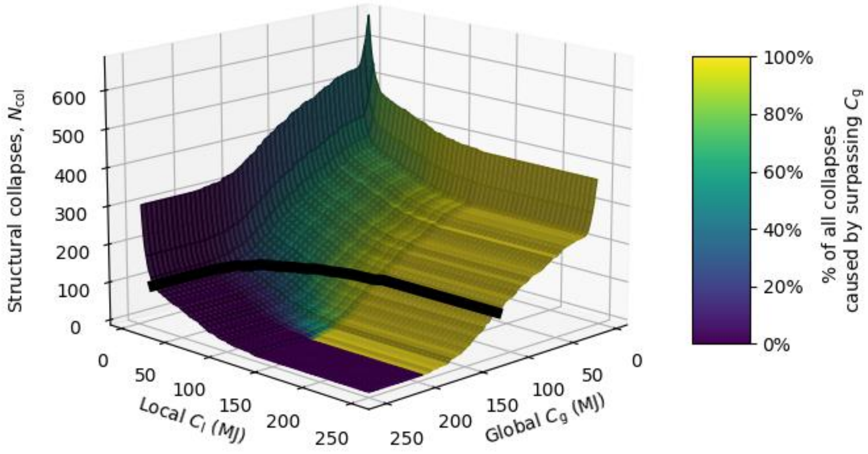

Figure 4-10. Number of collapses, $N_{collapse}$, as a 3D surface in Scenario 1, depending on the C_l and C_g. The black line represents where the surface overlaps with the Norwegian criterion (1 structural failure every 10^4 years). Figure reused from Paper IV.

A summary of the probability of collapse, with C_l set to 50 MJ and C_g set to 160 MJ, is presented in Table 4-12. Figure 4-11 illustrates the minimum combination in each scenario for how C_l and C_g could be varied to comply with the Norwegian criterion of 10^{-4}.

Table 4-12. The probability of collapse (N_{col}/Y_{rep}) with C_l set to 50 MJ and C_g set to 160 MJ.

	Scenario 1	**Scenario 2**	**Scenario 3**	**Scenario 4**	**Scenario 5**
Probability of collapse	0.81×10^{-4}	0.78×10^{-4}	1.66×10^{-4}	0.67×10^{-4}	1.13×10^{-4}

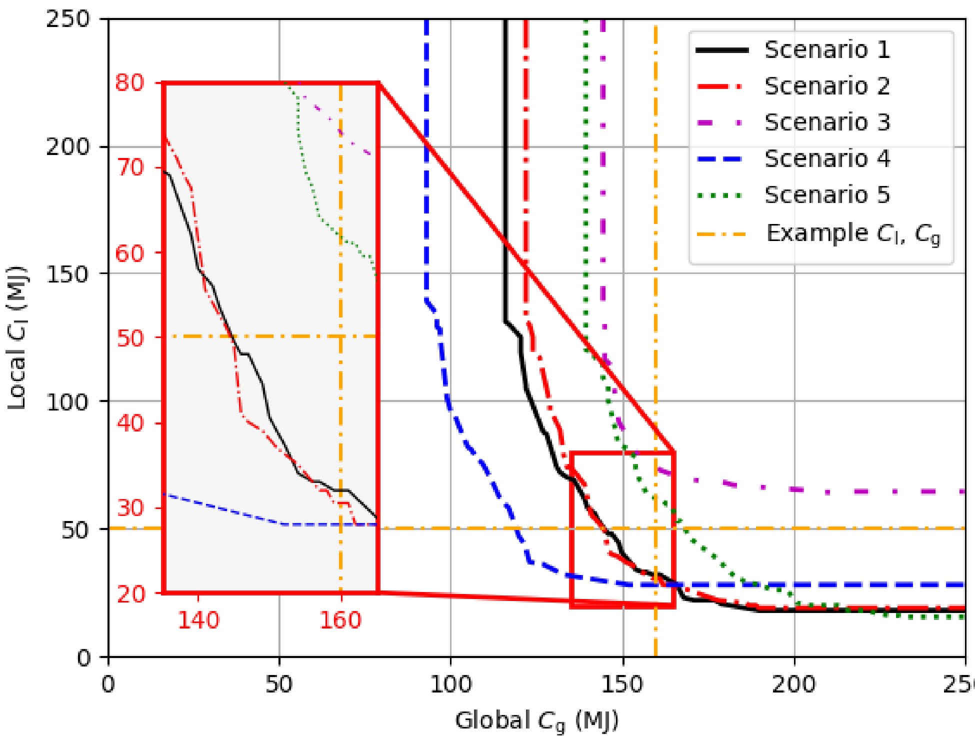

Figure 4-11. The combination of minimum strength with regard to local and global strength, for a collapse rate of 10^{-4}. "An unsafe design" occurs when a scenario crosses above-right of the C_l and C_g lines, as for Scenarios 3 and 5. Figure reused from Paper IV.

Even though Scenario 2 resulted in more simulated allisions than Scenario 1 (1,035 compared to 1,007), the probability of collapse was slightly lower (0.78×10^{-4} compared to 0.81×10^{-4}). This surprising outcome was caused by the Monte Carlo simulation of input parameters: in Scenario 2, there were generally more allisions, which generated higher global damage compared to Scenario 1, but allisions of around 160 MJ occurred more frequently in Scenario 1.

Table 4-12 and Figure 4-11 illustrate that, with the given C_l and C_g, Scenarios 1, 2, and 4 fell within the Norwegian criterion: they were constantly to the left and under the orange lines of the set values of C_l and C_g in Figure 4-11, and therefore the probability of collapse was less than 1×10^{-4} per year. However, Scenarios 3 and 5 were partly to the right and above these lines, and the results presented in Table 4-12 illustrate that the probability of collapse was greater than 1×10^{-4} per year.

4.5.2 Concluding remarks

This study introduced the STAPS-cons methodology, a unified framework for assessing ship-bridge allision risk by integrating both probability and consequence assessments into a single methodology. One of the main strengths of this methodology lies in its ability to evaluate the risk of bridge collapse while accounting for navigational, hydrodynamical, and structural design factors. This unified methodology enables a holistic view which supports informed decision-making. Although the methodology requires the analysis of a large quantity of AIS data along with advanced simulations, it reduces uncertainties in the analysis by addressing multiple risk components simultaneously.

The results of Paper IV showed that three of the five scenarios met the Norwegian threshold for acceptable collapse probability ($<10^{-4}$ per year), which highlights how the method can be applied. The study also underscores the importance of accurately modelling failure durations, such as the time for *miss of turning points*, which had a major impact on the required structural strength of the bridge. Overall, STAPS-cons represents an advancement in maritime risk assessment, offering a robust and comprehensive methodology for managing allision risks from ships.

While the STAPS-cons methodology reduces uncertainty by integrating multiple components of risk, it is important to acknowledge that uncertainties remain—particularly in the assumptions and simplifications made during the modelling. These include the extrapolation of failure statistics from AIS data and the autopilots' representation of ship behaviour in fast-time simulations. However, the methodology has already demonstrated sensitivity to such uncertainties, notably through the variation of failure probabilities and durations in both this paper and in Paper I. These analyses illustrate how modelling assumptions influence the estimated risk, and they provide a foundation for assessing the robustness of the results. Further refinement of uncertainty treatment, such as expanding the data scope or formalising confidence intervals for the rare failures, could enhance transparency.

5 Conclusions

This chapter presents the main findings and conclusions of the thesis, along with potential applications in related fields. The aim of this research was to study methods for ship-bridge allisions and to offer enhancements of currently commonly-used methods. The study resulted in the development of a novel methodology for assessing the risk of ship-bridge allisions. Three objectives for the development of this methodology were defined:

(i) Develop methods which can quantify different types of ship failure events in terms of both frequency and duration.
(ii) Propose a methodology which uses ship failure events in a maritime probability assessment context.
(iii) Combine the probabilistic methodology with a consequence model to assess the risk of allisions.

The first objective was accomplished through the research presented in Papers I and II, where five failure types were identified and classified. The second objective was fulfilled by the research presented in Paper III, where the identified failure types were integrated into the Ship Traffic Allision Probability using Monte Carlo Simulations (STAPS) methodology. The third objective was achieved in the research presented in Paper IV, where consequence modelling was incorporated into the STAPS framework to result in the STAPS-cons methodology.

The development of the STAPS-cons methodology was made possible by advances in Automatic Identification System (AIS) technology and Maritime Manoeuvring Simulators (MMS), which reduce the subjectivity and thus enable the realistic modelling of ship behaviour and failure scenarios. Earlier foundational work by Fujii and Macduff in the 1970s, and later work by Pedersen, relied on simplified geometric models and closed-form equations, such as those presented in Equations (2.1) – (2.3); these models laid the groundwork for maritime risk assessment, but they were constrained by the limited data and computational tools available at the time. By contrast, STAPS-cons builds on modern simulation capabilities and location-specific failure data to derive probabilities directly from ship manoeuvring simulations, where each simulation can be replayed and analysed. This approach was found to enable more detailed assessments, support the evaluation of risk mitigation strategies, and integrate both probability and consequence modelling into a single framework. This methodological advancement opens new possibilities for research in maritime risk and infrastructure resilience.

A notable strength of the STAPS-cons methodology is its ability to assess uncertainty by incorporating location-specific failure data and simulating a wide range of scenarios. As concluded in Papers I, III, and IV, the input parameters are sensitive, and it is important to define them as realistically as possible. Paper III demonstrated that the amount of influence an input parameter has on the allision probability depends on the model layout. This was specifically shown in two case studies where allision risk was determined both by STAPS-cons and the most used software for quantitative maritime risk assessments, IWRAP Mk II: for layouts where parts of the ship route are directed towards the bridge, the failure duration of *miss* *of turning point* (STAPS) and that of *mean time between checks* (IWRAP Mk II) are particularly important to define correctly, whereas these parameters may have negligible impact for layouts without such routes. This finding highlights the importance of carefully reviewing the model layout to identify which parameters will have the most significant effect in the risk assessment. The research also concluded that the STAPS-cons methodology was suitable for suggesting and assessing risk mitigation options. Furthermore, a user sensitivity study in which ten experts defined future ship route coordinates revealed substantial variation in allision probabilities, highlighting the need to study the model layout itself as a key factor in risk modelling.

The developed STAPS-cons methodology shares similarities with other existing models for assessing ship allision risk. For instance, the MTS simulations by Ulusçu et al. (2009) and van Dorp and Merrick (2011) are capable of identifying rare events, a feature also supported by STAPS-cons. No direct comparison was made between STAPS-cons and the SAMSON software; however, since the findings by ABL and MARINE (2024) showed comparable results for IWRAP Mk II and SAMSON, it is assumed that a comparison between STAPS and SAMSON would result in similar conclusions as the STAPS comparison with IWRAP Mk II. One point worth noting is that SAMSON includes the *Wrong Course at the Turning point* (WCT) failure type, which is not modelled in IWRAP Mk II but is included in the simulations in STAPS.

This research contributes by bridging the gap between probabilistic modelling and consequence analysis with a single maritime risk methodology. This methodology offers value to a range of stakeholders: bridge designers can use it to evaluate structural resilience; maritime authorities can apply it to assess navigational risks and risk mitigation options; and policymakers can utilise its integrated risk approach to support strategic decisions regarding infrastructure investments and regulatory development.

5.1 Scientific contributions and novelty

This thesis provides several scientific contributions which advance the field of maritime risk assessment, particularly in the context of analysing the risk of ship-bridge allisions:

Development of an integrated risk assessment framework

- The STAPS-cons methodology unites probabilistic modelling and consequence analysis within a single framework. This enables a more comprehensive and realistic assessment of allision risk than approaches which treat these components separately.

Use of location-specific failure statistics derived from AIS data

- Five distinct failure types were identified and quantified based on AIS data and real-world ship trajectories. This approach enhances the accuracy of the analysis by incorporating locally observed failure behaviours and durations.

Application of large-scale Monte Carlo simulations in manoeuvring scenarios

- Millions of simulations were conducted to model ship behaviour under failure conditions and to estimate accident probabilities. This supports robust statistical analysis and the identification of high-risk scenarios.

Coupling with nonlinear FEA for consequence modelling

- Although no FEA simulations were performed in this thesis, the developed methodology can use such simulations to assess the probability of bridge collapse. This facilitates the evaluation of design alternatives and risk mitigation strategies.

These contributions represent a significant advancement in maritime risk modelling by leveraging modern simulation capabilities and empirical data to produce more context-sensitive assessments.

6 Future work

This thesis has presented a novel methodology for assessing the risk of ship-bridge allisions. Several areas for future research to enhance and expand the developed STAPS-cons methodology are proposed in this chapter.

While the primary objective of this thesis was to develop a methodology for assessing the risk of ship-bridge allisions, the proposed methodology could also be applied in other domains. One example is evaluating the allision risk for offshore wind farms, for which demand has increased during the research for this PhD and to which the STAPS-cons methodology can be applied without modification. Similarly, the STAPS methodology could be adapted to assess the probability of ship groundings; however, the consequence modelling for groundings differs substantially from that of allisions and would therefore require a separate modelling approach tailored to the specific characteristics of grounding events.

Because the methodology developed in this thesis relies on an autopilot to follow predefined routes in open waters, its ability to simulate tight navigation scenarios at variable speeds is limited. Nevertheless, the autopilot commands could be replaced with real-time navigator inputs from a simulation, to enhance realism in the manoeuvring. An important difference between autopilot runs and real-time navigators is the impact of environmental conditions. The autopilot can compensate for environmental effects to maintain the route; however, issuing the same commands under different environmental conditions results in different outcomes, which gives rise to a large matrix of vessel types and environmental scenarios to run in real-time. Additionally, the failure behaviours may need to be adapted to suit these simulations. Despite these challenges, integrating real-time simulation represents a promising avenue for extending the methodology, and it highlights the potential for another use case in a similar field.

The process of establishing failure statistics (specifically in terms of frequency and duration) currently involves time-consuming and somewhat subjective manual work. Due to time constraints, it was not possible in this thesis to develop or train an AI model to automatically identify such anomalies. Future research could explore the use of AI to automate the process of identifying anomalies, thereby reducing both the time required for and the subjectivity involved in classifying failure events. With the identification of more failure events, it would also be possible to conduct deeper analyses of the failure durations and of whether normal and lognormal distributions fit these times best.

In Paper III, ten experts were invited to offer suggestions on how future ship routes could change due to a new bridge. The study revealed that the user selection of route coordinates had a major impact on the estimated allision probability. To overcome this user sensitivity, it would be beneficial to add route coordinates automatically. Rong et al. (2022) proposed a clustering technique using AIS data to generate and predict routes based on existing waterways; developing a similar technique which is also capable of predicting future route changes due to regulations or restrictions of the waterway remains an open area for further investigation.

In Paper IV, five nonlinear FEA simulations were used to assess the deformation and the distribution of energy of all allisions. However, it would be preferable if the fast-time simulation could approximate the deformation energy itself. Efforts to this end were made in the research for this thesis, using a small timestep and calculating allision forces based on the overlapping area (of the ship and the structure) multiplied by a pressure. These attempts were not successful, since the modelling of pressure distribution across different parts of the ship and the structure could not be validated within the timeframe of this research. Thus, developing and validating such a model for use in fast-time simulations is recommended for future work.

The definition of a general probability criterion is also a subject for further discussion, as it does not account for the severity of a bridge collapse. Johansen and Askeland (2019) proposed the use of an F-N curve to better represent both the probability and the consequences of an event, measured in terms of potential loss of life; this approach enables the integration of risk acceptance and design criteria. Despite the current absence of such a definition in Sweden and Denmark, establishing a suitable, context-sensitive risk criterion remains another important area for future research. Furthermore, with regard to the risk criterion, it is important to define the safety margins. Papers I and III set a 5% threshold, assumed for different seeds, in the Monte Carlo simulation; defining a similar threshold for the safety margin with the included consequence assessment is another path for future research.

7 References

AASHTO, 2009. Guide specifications and commentary for vessel collision design of highway bridges, 2nd ed. *American Association of State Highway and Transportation Officials* (AASHTO), U.S.

Abaqus, 2023. [WWW Document]. *Dassault Systèmes*. URL https://www.3ds.com/products/simulia/abaqus (accessed 2025-11-01).

ABL, MARINE, 2024. SN10 Phase II Navigational Risk Modelling: *ABL and MARIN Joint Technical Memo.* Ad Hoc Study Group SN10 FSA. Report No. HHR22475-R0009.

Ahnert, K., Mulansky, M., 2024. Numeric Odeint. Software version 1.84.0. [WWW Document]. *Boost software*. URL https://www.boost.org/doc/libs/1_84_0/libs/numeric/odeint/doc/html/index.html (accessed 2025-11-01).

Amdahl, J., 1983. Energy absorption in ship-platform impacts. Doctoral Thesis at Department of Marine Technology – *The Norwegian Institute of Technology, University of Trondheim*. UR-83-34.

Ansys, 2024. Ansys LS-DYNA [WWW Document]. *Ansys Inc.* URL https://www.ansys.com/products/structures/ansys-ls-dyna (accessed 2025-11-01).

Antão, P., Sun, S., Teixeira, A.P., Soares, C.G., 2023. Quantitative assessment of ship collision risk influencing factors from worldwide accident and fleet data. *Reliability Engineering & System Safety*, 234 (June 2023), 109166. https://doi.org/10.1016/j.ress.2023.109166.

AP News, 2024. Maryland officials release timeline, cost estimate, for rebuilding bridge [WWW Document]. *AP News*. URL https://apnews.com/article/baltimore-bridge-collapse-body-found-cdd8441c5dff48028d1e141b943ca31e (accessed 2025-11-01).

Bjøndal, L.H., Andersson (NKA Hörteborn), A., Forsman, B., Wilske, E., 2016. Ship Collision Risk Analysis for the Planned Crossing of Bjornafjorden, in: *Proceedings of the 7th International Conference on Collision and Grounding of Ships and Offshore Structures (ICCGS 2016)*, 15-18 June, 2016, Ulsan, Korea, p. 29–34.

BMA and DMA, 2005. Collision with the Great Belt West Bridge 3 March 2005. Report, DMA case: 200502332, BMA case: 8000614/2005/5127. Issued on 17 August 2005. [WWW Document]. URL https://www.bahamasmaritime.com/wp-content/uploads/2020/10/BMA-Investigation-Report-Allision-between-the-Karen-Danielsen-and-the-Great-Belt-West-Bridge-.pdf?swcfpc=1 (accessed 2025-11-01).

Braestrup, M.W., 2012. Eurocodes applied to the Øresund Link between Denmark and Sweden. *Structural Engineering International*, 22, p.246–249. https://doi.org/10.2749/101686612X13291382990723.

CEN, 2006. Eurocode 1: Actions on structures - Part 1-7: General actions - Accidental actions (No. 305/2011), European standard EN 1991-1-7. *European Committee for Standardization*, Brussels, Belgium.

Chen, T.L., Cheng, Y.H., Wu, H., 2024. A simplified simulation strategy for barge-bridge collision learned from collapse of Taiyangbu Bridge. *Engineering Structures,* 303 (15 March 2024), 117592. https://doi.org/10.1016/j.engstruct.2024.117592.

Chen, L., Yan, X., Huang, L., Yang, Z., Wang, J., 2018. A systematic simulation methodology for LNG ship operations in port waters: A case study in Meizhou Bay. *Journal of Marine Engineering & Technology*, 17, p. 12–32. https://doi.org/10.1080/20464177.2016.1276823.

Čorić, M., Mandžuka, S., Gudelj, A., Lušić, Z., 2021. Quantitative ship collision frequency estimation models: A review. *Journal of Marine Science and Engineering*, 9 (5), 533. https://doi.org/10.3390/jmse9050533.

COWI, 2008. Risk analysis of sea traffic in the area around Bornholm. *COWI A/S*, Kongens Lyngby, Denmark, Tech. Rep. P-65775-002.

Cucinotta, F., Guglielmino, E., Sfravara, F., 2017. Frequency of ship collisions in the Strait of Messina through Regulatory and environmental constraints assessment. *Journal of Navigation* 70 (5), p. 1002–1022. https://doi.org/10.1017/S0373463317000157.

Dugan, S.A., Utne, I.B., 2023. Evaluating differences between maritime accident databases. Presented at the European Safety and Reliability Conference, (ESREL 2023), 3-8 September 2023, Southampton, UK. *Research Publishing*, Singapore. https://doi.org/10.3850/978-981-18-8071-1_P191-cd.

Eidem, M.E., Sha, Y., Moen, I., Flage, R., 2023. Ship allision risk analysis for the 28-year-old Nordhordland bridge in Norway. Presented at the European Safety and Reliability Conference, (ESREL 2023), 3-8 September 2023, Southampton, UK. *Research Publishing*, Singapore, p. 112–119. https://doi.org/10.3850/978-981-18-8071-1_P183-cd.

Engberg, P.C., 2017. IWRAP Mk II v5.3.0 manual (No. 5.3). *GateHouse A/S, IALA*. [WWW Document] Theory guideline. URL https://www.iala.int/wiki/iwrap/images/7/75/IWRAP_Mk2_Manual_v5.3.pdf (accessed 2025-11-01).

European Marine Casualty Information Platform (EMCIP), 2023. [WWW Document]. *EMCIP Portal*. URL https://portal.emsa.europa.eu/emcip-public/#/public-occurrences (accessed 2025-11-01).

Fan, C., He, X., Huang, L., Li, H., Wen, T., 2024. Research on collision warning method for ship-bridge based on safety potential field. *Applied Sciences*, 14 (19), 9089. https://doi.org/10.3390/app14199089.

Fan, S., Yang, Z., 2024. Accident data-driven human fatigue analysis in maritime transport using machine learning. *Reliability Engineering & System Safety*, 241 (January 2024), 109675. https://doi.org/10.1016/j.ress.2023.109675.

Friis-Hansen, P., 2008. Basic modelling principles for prediction of collision and grounding frequencies, Rev. 4: 2008.03.09. [WWW Document]. IWRAP Mk II Working Document. URL https://www.iala.int/wiki/iwrap/images/2/2b/IWRAP_Theory.pdf (accessed 2025-11-01).

Fujii, Y., 1983. Integrated study on marine traffic accidents, in: *IABSE Colloquium on Ship Collision with Bridges and Offshore Structures*, Volume 42. Copenhagen 1983. p. 91–98.

Fujii, Y., Shiobara, R., 1971. The analysis of traffic accidents. *Journal of Navigation*, 24 (4), p. 534–543. https://doi.org/10.1017/S0373463300022372.

Fujii, Y., Tanaka, K., 1971. Traffic capacity. *Journal of Navigation*, 24 (4), p. 543–552. https://doi.org/10.1017/S0373463300022384.

Galić, S., Lušić, Z., Mladenović, S., Gudelj, A., 2022. A chronological overview of scientific research on ship grounding frequency estimation models. *Journal of Marine Science and Engineering*, 10 (2), 207. https://doi.org/10.3390/jmse10020207.

Gan, L., Gao, Z., Zhang, X., Xu, Y., Liu, R.W., Xie, C., Shu, Y., 2025. Graph neural networks enabled accident causation prediction for maritime vessel traffic. *Reliability Engineering & System Safety*, 257 (Part A, May 2025), 110804. https://doi.org/10.1016/j.ress.2025.110804.

GISIS, I., 2023. Global Integrated Shipping Information System [WWW Document]. URL https://gisis.imo.org/Public/MCI/Search.aspx?Mode=Advanced (accessed 2025-11-01).

Guo, S., Bolbot, V., Valdez Banda, O., 2024. An adaptive trajectory compression and feature preservation method for maritime traffic analysis. *Ocean Engineering*, 312 (Part 2, 15 November 2024), 119189. https://doi.org/10.1016/j.oceaneng.2024.119189.

Guo, J., Qiu, L., Wu, J., Wang, J., 2022. Probability analysis of aberrant ship collision with sea-crossing bridges considering wind and current. *Journal of Bridge Engineering*, 27 (11), 04022108. https://doi.org/10.1061/(ASCE)BE.1943-5592.0001958.

Haris, S., 2013. Damage interaction analysis of ship collisions., Doctoral Thesis at Department of Marine Technology – *The Norwegian Institute of Technology*, University of Trondheim. 2023:208. ISBN: 978-82-471-4531-9.

Harris, C.R., Millman, K.J., van der Walt, S.J., Gommers, R., Virtanen, P., Cournapeau, D., Wieser, E., Taylor, J., Berg, S., Smith, N.J., Kern, R., Picus, M., Hoyer, S., van Kerkwijk, M.H., Brett, M., Haldane, A., del Río, J.F., Wiebe, M., Peterson, P., Gérard-Marchant, P., Sheppard, K., Reddy, T., Weckesser, W., Abbasi, H., Gohlke, C., Oliphant, T.E., 2020. Array programming with NumPy. *Nature*, 585, p. 357–362. https://doi.org/10.1038/s41586-020-2649-2.

Hörteborn, A., 2024. Allision modelling in IWRAP Mk II–A verification and sensitivity study, in: *Advances in the Collision and Grounding of Ships and Offshore Structures. (ICCGS 2023)*, 11-13 September, 2023, Nantes, France. CRC Press, p. 51–59. https://doi.org/10.1201/9781003462170.

Hörteborn, A., 2025. OMRAT. [WWW Document]. Github repository URL https://github.com/axelande/OMRAT (accessed 2025-11-01).

Hörteborn, A., 2021. Ship Behaviour and Ship-Bridge Allision Analysis. Licentiate thesis at Department of Mechanics and Maritime Sciences - *Chalmers University of Technology*. Report No 2021:02.

Hörteborn, A. & Eidem, M. E., 2025. Probability of active navigational failure. *Journal of Navigation*, Accepted. https://doi.org/10.1017/S0373463325101100.

Hörteborn, A. & Ringsberg, J. W., 2021. A method for risk analysis of ship collisions with stationary infrastructure using AIS data and a ship manoeuvring simulator. *Ocean Engineering*, 235 (1 September 2021), 109396, ISSN: 0029-8018. https://doi.org/10.1016/j.oceaneng.2021.109396.

Hörteborn, A.; Ringsberg, J. W.; Wengang, M. & Lundbäck, O., 2025. Probabilistic analysis of ship-bridge allisions when designing bridges. *Reliability Engineering & System Safety*, 260 (August 2025), 111026. DOI: https://doi.org/10.1016/j.ress.2025.111026.

Hörteborn, A.; Sha, Y.; Ringsberg, J. W.; Lundbäck, O. & Mao, W., 2025. Risk analysis methodology for ship-bridge allisions – A combined probability and consequence analysis. *Engineering Structures*, Accepted.

IHS Fairplay, 2023. Sea-web Casualty & Events [WWW Document]. URL https://maritime.ihs.com/ (accessed 2025-11-01).

IMO, 2010. Degree of Risk Evaluation (No. SN. 1 /Circ.296). *IMO*, London.

IMO, 1998. RESOLUTION MSC.74(69), MSC. *IMO*, London.

ITU-R, 2014. Technical characteristics for an automatic identification system using time division multiple access in the VHF maritime mobile frequency band (Recommendation No. M.1371-5), M Series. *International Telecommunication Union*, Geneva.

Jin, Y., Sha, Y., Moan, T., 2020. Risk Analysis of a floating bridge subjected to ship collisions (Restricted No. 2020xxyy). NTNU for *Norwegian Public Road Administration*, Trondheim, Norway.

Johansen, I.L., Askeland, T., 2019. Risk acceptance criteria for extreme fjord crossings, in: *IABSE Symposium*, Guimaraes 2019: Towards a Resilient Built Environment Risk and Asset Management - Report. (IABSE 2019). 27–29 March, 2019, Portugal. IABSE Symposium Guimarães 2019, p. 1402–1409. https://doi.org/10.2749/guimaraes.2019.1402.

Johansen, T.A., Perez, T., Cristofaro, A., 2016. Ship collision avoidance and COLREGS compliance using simulation-based control behavior selection with predictive hazard assessment. *IEEE Transactions on Intelligent Transportation Systems*, 17 (12), p. 3407–3422. https://doi.org/10.1109/TITS.2016.2551780.

Karlsson, M., Rasmussen, F.M., Frisk, L., Ennemark, F., 1998. Verification of ship collision frequency model. *Proceedings of the international symposium on advances in ship collision analysis*, 10-13 May 1998 Copenhagen, Denmark. p. 117–121. ISBN: 9789054109624.

Korupoju, A.K., Kapadia, V., Vilwathilakam, A.S., Samanta, A., 2025. Ship Collision Risk Evaluation using AIS and weather data through fuzzy logic and deep learning. *Ocean Engineering*, 318 (15 February 2025), 120116. https://doi.org/10.1016/j.oceaneng.2024.120116.

Kowalska, K., Peel, L., 2012. Maritime anomaly detection using Gaussian process active learning, in: 2012 *15th International Conference on Information Fusion. IEEE*, 09-12 July 2012 Singapore. IEEE, p. 1164–1171. ISBN: 978-0-9824438-5-9.

Kretschmann, L., 2020. Leading indicators and maritime safety: Predicting future risk with a machine learning approach. *Journal of Shipping and Trade*, 5, 19. https://doi.org/10.1186/s41072-020-00071-1.

Kulendorf, Y., Van der Tak, C., Others, 2019. Samson: Technical documentation version 3.1.1, [Report] 27 March 2019. *MARIN*, Report No. 30751-4- MSCN- rev. 02.

Ladeira, I., Márquez, L., Echeverry, S., Le Sourne, H., Rigo, P., 2023. Review of methods to assess the structural response of offshore wind turbines subjected to ship impacts. *Ships and Offshore Structures*, 18 (6), p. 755–774. https://doi.org/10.1080/17445302.2022.2072583.

Laheld, P., 1983. Statistics on collision accidents involving offshore structures, in: *IABSE Colloquium on Ship Collision with Bridges and Offshore Structures*, Copenhagen 1983. Volume 42, p. 27–45. https://doi.org/10.5169/seals-31653.

Larsen, O.D., 1993. Ship collision with bridges: The interaction between vessel traffic and bridge structures. *IABSE 1993*. ISBN: 3857480793, 9783857480799.

Larsen, O.D., 1983. Ship collision risk assessment for bridges, in: *IABSE Colloquium on Ship Collision with Bridges and Offshore Structures,* Copenhagen 1983. Volume 42, p. 113–128. https://doi.org/10.5169/seals-31658.

Laxhammar, R., 2008. Anomaly detection for sea surveillance, in: *2008 11th International Conference on Information Fusion*. Cologne, Germany, 30 June - 03 July 2008. IEEE. ISBN: 978-3-8007-3092-6.

Le Sourne, H., Besnard, N., Cheylan, C., Buannic, N., 2012. A ship collision analysis program based on upper bound solutions and coupled with a large rotational ship movement analysis tool. *Journal of Applied Mathematics*, 2012, 375686. https://doi.org/10.1155/2012/375686.

Liu, C., Zhang, S., Cao, L., Lin, B., 2023. The identification of ship trajectories using multi-attribute compression and similarity metrics. *Journal of Marine Science and Engineering*, 11 (10), 2005. https://doi.org/10.3390/jmse11102005.

Liu, J., Zhang, J., Yan, X., Soares, C.G., 2022. Multi-ship collision avoidance decision-making and coordination mechanism in Mixed Navigation Scenarios. *Ocean Engineering*, 257 (1 August 2022), 111666. https://doi.org/10.1016/j.oceaneng.2022.111666

Macduff, T., 1974. The probability of vessel collisions. *Ocean Industry*, 9, p. 144–148.

Márquez, L., Le Sourne, H., Rigo, P., 2022. Mechanical model for the analysis of ship collisions against reinforced concrete floaters of offshore wind turbines. *Ocean Engineering*, 261 (1 October 2022), 111987. https://doi.org/10.1016/j.oceaneng.2022.111987.

Minorsky, V.U., 1958. An analysis of ship collisions with reference to protection of nuclear power plants. *George G. Sharp Inc.*, New York. OSTI ID: 4257123.

Moore, G., 1965. Moore’s law. *Electronics Magazine*, 38 (8), April 19, 1965.

Munim, Z.H., Sørli, M.A., Kim, H., Alon, I., 2024. Predicting maritime accident risk using Automated Machine Learning. *Reliability Engineering & System Safety*, 248 (August 2024), 110148. https://doi.org/10.1016/j.ress.2024.110148.

NBC4, 2024. The White House wants $4 billion to rebuild Key Bridge in Baltimore and respond to other disasters. [WWW Document] *NBC4 Washington*. URL https://www.nbcwashington.com/news/local/the-white-house-wants-4-billion-to-rebuild-key-bridge-in-baltimore-and-respond-to-other-disasters/3652620/?os=fuzzsc...&ref=app (accessed 2025-11-01).

New York Times, 1977. New Bridge Bypasses The Baltimore Tunnel. *The New York Times*. 27 March 1977, p. 23.
Norrbin, N.H., 1965. Forces in oblique towing of a model of a cargo liner and a divided double body geosim, in: Meddelanden Från Statens Skeppsprovningsanstalt. *Scandinavian University Books*, Gothenburg, Sweden.
NTSB, 2024. Contact of Containership Dali with the Francis Scott Key Bridge and Subsequent Bridge Collapse. *National Transportation Safety Board*, Report No. DCA24MM031.
Orcina, L., 2022. OrcaFlex user manual: OrcaFlex version 11.2 c. *Daltongate Ulverston Cumbria*, UK.
Pan, J., Wang, Y., Wang, T., Xu, M., 2024. Study on assessment of collision probability between ship and bridge based on Automatic Identify System data. *Journal of Marine Science and Engineering*, 12 (3), 452. https://doi.org/10.3390/jmse12030452.
Pedersen, P.T., 2010. Review and application of ship collision and grounding analysis procedures. *Marine Structures*, 23 (3), p. 241–262. https://doi.org/10.1016/j.marstruc.2010.05.001
Pedersen, P.T., 1995. Collision and grounding mechanics. Presented at the WEMT'95: Proceedings of Ship Safety and Protection of the Environment - From a Technical Point-of-View, *Danish Society of Naval Architecture and Marine Engineering*, Copenhagen, Denmark, p. 125–157.
Pedersen, P.T., Chen, J., Zhu, L., 2020. Design of bridges against ship collisions. *Marine Structures*, 74 (November 2020), 102810. https://doi.org/10.1016/j.marstruc.2020.102810.
Pedersen, P.T., Jensen, J.J., 1991. Ship impact analysis for bottom supported offshore structures, *Advances in Marine Structures 2nd Intl Conference*, 21-24 May 1991; Dunfermline, Scotland, U.K. p. 276–296.
Pedersen, P.T., Valsgård, S., Olsen, D., Spangenberg, S., 1993. Ship impacts: Bow collisions. *International Journal of Impact Engineering*, 13, p. 163–187. https://doi.org/10.1016/0734-743X(93)90091-K.
Pedersen, P.T., Zhang, S., 1998. On impact mechanics in ship collisions. *Marine Structures*, 11 (10), p. 429–449. https://doi.org/10.1016/S0951-8339(99)00002-7.
Persson, G., Rosengren, B., 2000. Villkoren för järnvägstrafiken på den fasta förbindelsen över Öresund m.m. Prop. 1999/2000:66. *Swedish Government*.
Petersen, M.J., Pedersen, P.T., 1981. Collisions Between Ships and Offshore Platforms. *Presented at the Offshore Technology Conference*, Houston, Texas, May 1981. pp. OTC-4134-MS. https://doi.org/10.4043/4134-MS.
Poschmann, P., Wilko, B., 2017. European Maritime Simulator Network (EMSN) Integration Test Report (No. 3.15c). [WWW Document] Project report URL https://s3-eu-west-1.amazonaws.com/stm-stmvalidation/uploads/20200225090057/STMVal_D3.15-EMSN-Integration-Test-Report.pdf (accessed 2025-11-01).
Pyman, M.A.F., Austin, J.S., Lyon, P.R., 1983. Ship/platform collision risk in the UK sector, in: *IABSE Colloquium on Ship Collision with Bridges and Offshore Structures*, Copenhagen 1983, Volume 42, p. 145–152. https://doi.org/10.5169/seals-32413.

Rasmussen, F.M., Glibbery, K.A.K., Melchild, K., Hansen, M.G., Jensen, T.K., Lehn-Schiøler, T., Randrup-Thomsen, S., 2012. Quantitative assessment of risk to ship traffic in the Fehmarnbelt fixed link project. *Journal of Polish Safety and Reliability Association*, 3 (1), p. 123–134.

Ren, Y., Meng, Q., Chen, C., Hua, X., Zhang, Z., Chen, Z., 2022. Dynamic behavior and damage analysis of a spar-type floating offshore wind turbine under ship collision. *Engineering Structures*, 272 (1 December 2022), 114815. https://doi.org/10.1016/j.engstruct.2022.114815.

Ringsberg, J.W., Amdahl, J., Chen, B.Q., Cho, S.-R., Ehlers, S., Hu, Z., Kubiczek, J.M., Kõrgesaar, M., Liu, B., Marinatos, J.N., 2018. MARSTRUCT benchmark study on nonlinear FE simulation of an experiment of an indenter impact with a ship side-shell structure. *Marine Structures*, 59 (May 2018), p. 142–157. https://doi.org/10.1016/j.marstruc.2018.01.010.

RISE, 2025. SEAMAN simulations [WWW Document]. URL https://www.ri.se/en/expertise-areas/test-demo/seaman-simulations (accessed 2025-11-01).

Rong, H., Teixeira, A.P., Guedes Soares, C., 2024. A framework for ship abnormal behaviour detection and classification using AIS data. *Reliability Engineering & System Safety*, 247 (July 2024), 110105. https://doi.org/10.1016/j.ress.2024.110105.

Rong, H., Teixeira, A.P., Guedes Soares, C., 2022. Maritime traffic probabilistic prediction based on ship motion pattern extraction. *Reliability Engineering & System Safety*, 217 (January 2022), 108061. https://doi.org/10.1016/j.ress.2021.108061.

Rudan, S., Ćatipović, I., Berg, R., Völkner, S., Prebeg, P., 2019. Numerical study on the consequences of different ship collision modelling techniques. *Ships and Offshore Structures*, 14 (1), p. 387–400. https://doi.org/10.1080/17445302.2019.1615703.

Sánchez-Beaskoetxea, J., Basterretxea-Iribar, I., Sotés, I., Maruri Machado, M. de las M., 2021. Human error in marine accidents: Is the crew normally to blame? *Maritime Transport Research*, 2 (2021), 100016. https://doi.org/10.1016/j.martra.2021.100016.

Sha, Y., Amdahl, J., 2019. A simplified analytical method for predictions of ship deckhouse collision loads on steel bridge girders. *Ships and Offshore Structures*, 14 (1), p. 121–134. https://doi.org/10.1080/17445302.2018.1560881.

Sha, Y., Amdahl, J., Dørum, C., 2021. Numerical and analytical studies of ship deckhouse impact with steel and RC bridge girders. *Engineering Structures*, 234 (1 May 2021), 111868. https://doi.org/10.1016/j.engstruct.2021.111868.

Sha, Y., Amdahl, J., Dørum, C., 2019a. Local and global responses of a floating bridge under ship–girder collisions. *Journal of Offshore Mechanics and Arctic Engineering*, 141 (3), pp. OMAE-18-1003. https://doi.org/10.1115/1.4041992

Sha, Y., Amdahl, J., Liu, K., 2019b. Design of steel bridge girders against ship forecastle collisions. *Engineering Structures*, 196 (1 October 2019), 109277. https://doi.org/10.1016/j.engstruct.2019.109277.

Sha, Y., Amdahl, J., Yang, K., 2019c. An efficient approach for ship collision design of reinforced concrete pontoon walls. Presented at the IOP Conference Series: Materials Science and Engineering, *IOP Publishing*, p. 012038. https://doi.org/10.1088/1757-899X/700/1/012038.

Shen, H., Hashimoto, H., Matsuda, A., Taniguchi, Y., Terada, D., Guo, C., 2019. Automatic collision avoidance of multiple ships based on deep Q-learning. *Applied Ocean Research*, 86 (May 2019), p. 268–288. https://doi.org/10.1016/j.apor.2019.02.020.

Sjøfartsdirektoratet, 2023. Arkiv for ulykkesstatistikk [WWW Document]. *Sjøfartsdirektoratet* URL https://www.sdir.no/sjofart/ulykker-risiko-og-sikkerhet/ulykkesstatistikk/arkiv-for-ulykkesstatistikk/ (accessed 2023-05-31).

Søreide, T.H., Amdahl, J., Eberg, E., Holmås, T., Hellan, Ø., 1993. USFOS—A computer program for progressive collapse analysis of steel offshore structures. Theory Manual, *SINTEF*, Trondheim, Norway.

sspasweden, 2020. PySim. *RISE Maritime Department* [WWW Document]. Github URL https://github.com/sspasweden/pysim (accessed 2025-11-01).

Statens Vegvesen, 2014. Håndbok N400 Bruprosjektering - Eurokodeutgave, in: Håndbok N400 Bruprosjektering - Eurokodeutgave. *Statens Vegvesen*.

Storheim, M., Jakobsen, S.E., Nedrebø, Ø.K., 2019. Preferred solution, K12 – Appendix J Ship collision. Report No. SBJ-33-C5-AMC-27-RE-110. *Statens Vegvesen*. [WWW Document] URL https://vegvesen.brage.unit.no/vegvesen-xmlui/handle/11250/2660035?show=full (accessed 2025-11-01).

Svanberg, M., Santén, V., Hörteborn, A., Holm, H., Finnsgård, C., 2019. AIS in maritime research. *Marine Policy*, 106 (August 2019), 103520. https://doi.org/10.1016/j.marpol.2019.103520.

Tabri, K., Määttänen, J., Ranta, J., 2008. Model-scale experiments of symmetric ship collisions. *Journal of Marine Science and Technology*, 13, p.71–84. https://doi.org/10.1007/s00773-007-0251-z.

Ugurlu, H., Cicek, I., 2022. Analysis and assessment of ship collision accidents using Fault Tree and Multiple Correspondence Analysis. *Ocean Engineering*, 245 (1 February 2022), 110514. https://doi.org/10.1016/j.oceaneng.2021.110514.

Ulusçu, Ö.S., Özbaş, B., Altıok, T., Or, İ., 2009. Risk analysis of the vessel traffic in the Strait of Istanbul. *Risk Analysis*, 29 (10), p. 1454–1472. https://doi.org/10.1111/j.1539-6924.2009.01287.x.

van Dorp, J.R., Merrick, J.R.W., 2011. On a risk management analysis of oil spill risk using maritime transportation system simulation. *Annals of Operations Research*, 187 (2011), p. 249–277. https://doi.org/10.1007/s10479-009-0678-1.

Virtanen, P., Gommers, R., Oliphant, T.E., Haberland, M., Reddy, T., Cournapeau, D., Burovski, E., Peterson, P., Weckesser, W., Bright, J. and Van Der Walt, S.J., 2020. SciPy 1.0: fundamental algorithms for scientific computing in Python. *Nature methods*, 17 (3), p. 261–272. https://doi.org/10.1038/s41592-019-0686-2.

Wang, C., Zhang, X., Gao, H., Bashir, M., Li, H., Yang, Z., 2024a. Optimizing anti-collision strategy for MASS: A safe reinforcement learning approach to improve maritime traffic safety. *Ocean & Coastal Management*, 253 (1 July 2024), 107161. https://doi.org/10.1016/j.ocecoaman.2024.107161.

Wang, Z., Sha, Y., Jakobsen, J.B., 2024b. Coupled Analysis of External Dynamics and Internal Mechanics in Ship-Floating Bridge Collision Studies, in: *OMAE2024. Volume 2: Structures, Safety, and Reliability*, pp. OMAE2024-123345. https://doi.org/10.1115/OMAE2024-123345.

Wang, Z., Sha, Y., Jakobsen, J.B., 2023. Floating bridge response under combined ship collision, wind and wave loads. *Ships and Offshore Structures*, (April 2023), p. 1–18. https://doi.org/10.1080/17445302.2023.2195242.

Weber, R., Olindersson, F., Olsson, F., 2019. Using a web-based simulation software in education, in: Using a Web-Based Simulation Software in Education, 20. Presented at *the Proceedings of the International Association of Maritime Universities, IAMU*, International Association of Maritime Universities, Tokyo, Japan, p. 150–157.

Xiao, F., Ma, Y., Wu, B., 2022. Review of probabilistic risk assessment models for ship collisions with structures. *Applied Sciences*, 12 (7), 3441. https://doi.org/10.3390/app12073441.

Xue, Y., Clelland, D., Lee, B.S., Han, D., 2011. Automatic simulation of ship navigation. *Ocean Engineering*, 38 (17–18), p. 2290–2305. https://doi.org/10.1016/j.oceaneng.2011.10.011.

Xue, J., Yang, P., Wang, Z., Li, Q., Hu, H., 2025. Cause analysis and management strategies for ship accidents: A Bayesian decision support model. *Ocean Engineering*, 320 (15 March 2025), 120291. https://doi.org/10.1016/j.oceaneng.2025.120291.

Yan, R., Mo, H., Yang, D., Wang, S., 2022. Development of denoising and compression algorithms for AIS-based vessel trajectories. *Ocean Engineering*, 252 (15 May 2022), 111207. https://doi.org/10.1016/j.oceaneng.2022.111207.

Ylitalo, J., 2010. Modelling Marine Accident Frequency (Master thesis). Aalto University, Espoo. https://aaltodoc.aalto.fi/handle/123456789/98008.

Yu, Z., Wang, X., Moan, T., Amdahl, J., Sha, Y., 2024. Ultimate and residual strength assessments of intact and collision damaged columns of the Bjørnafjorden floating bridge, in: *Advances in the Collision and Grounding of Ships and Offshore Structures. (ICCGS 2023)*, 11-13 September, 2023, Nantes, France. CRC Press, p. 387–393.

Zhang, M., Taimuri, G., Zhang, J., Zhang, D., Yan, X., Kujala, P., Hirdaris, S., 2025. Systems driven intelligent decision support methods for ship collision and grounding prevention: Present status, possible solutions, and challenges. *Reliability Engineering & System Safety*, 253 (January 2025), 110489. https://doi.org/10.1016/j.ress.2024.110489.

Zhang, S., Villavicencio, R., Zhu, L., Pedersen, P.T., 2017. Impact mechanics of ship collisions and validations with experimental results. *Marine Structures*, 52 (March 2017), p. 69–81. https://doi.org/10.1016/j.marstruc.2016.12.003.